Thermochemical Calculations Applied to High Temperature Corrosion of Ceramic and Refractory Materials

A. Kaiser

RWTH Aachen University
Department of Mineral Engineering
Chair of Ceramics and Refractories

High Temperature Corrosion

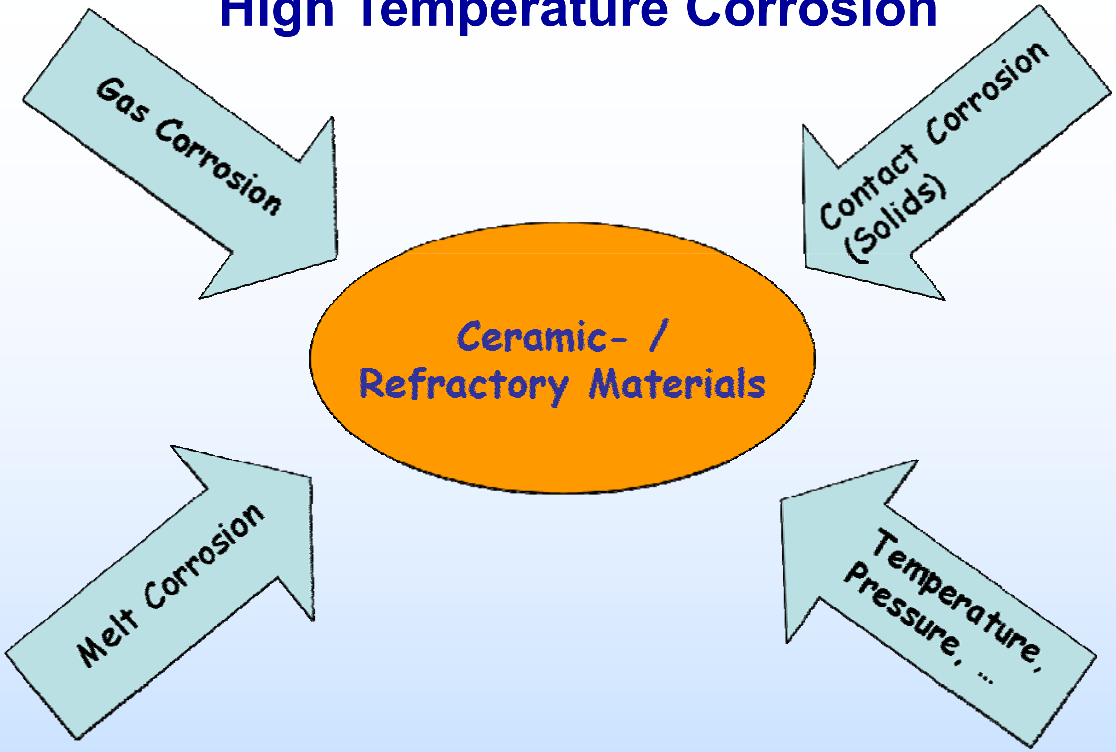

Thermochemical Calculations →

⇨ Prediction and analysis of corrosion processes
⇨ Prevention of corrosion processes by selection of suitable materials under given process conditions
⇨ Definition of application limits for specific materials
⇨ Optimization of high temperature processes → reduction of corrosion processes by optimization of relevant process parameters

Ceramic Tool Materials for the Shaping of Semi Solid Alloys

➢ Thixoforming

- Forming of Metals in the Semi-Solid State ($T_{Solidus} < T < T_{Liquidus}$)
- Alloy: Globulitic Solid Phase in a Low Melting Fluid Phase
- Thixotropic Flow Behaviour of Metal Alloy under Shear Stress during Forming
- Production of Complex Component Geometries with High Dimensional Accuracy Close to Final Dimensions

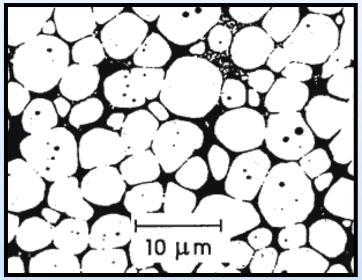

➢ Requirements for Ceramic Tool Materials:

- High Thermal Stability (850 - 1500 °C)
- High Strength and Wear Resistance
- High Thermal Shock Resistance
- Poor Wettability by Molten Alloys
- Good Corrosion Resistance

➡ Thermochemical Calculations

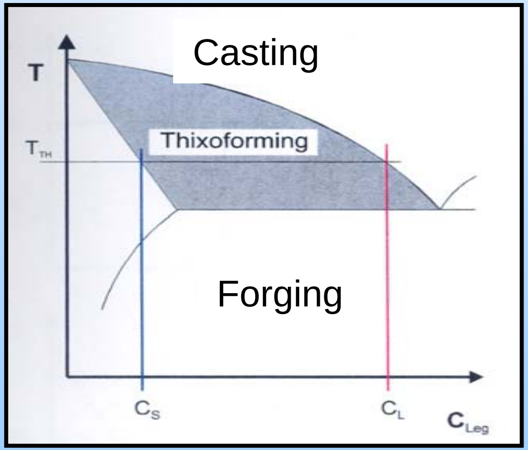

Corrosion Tests

Contact Corrosion

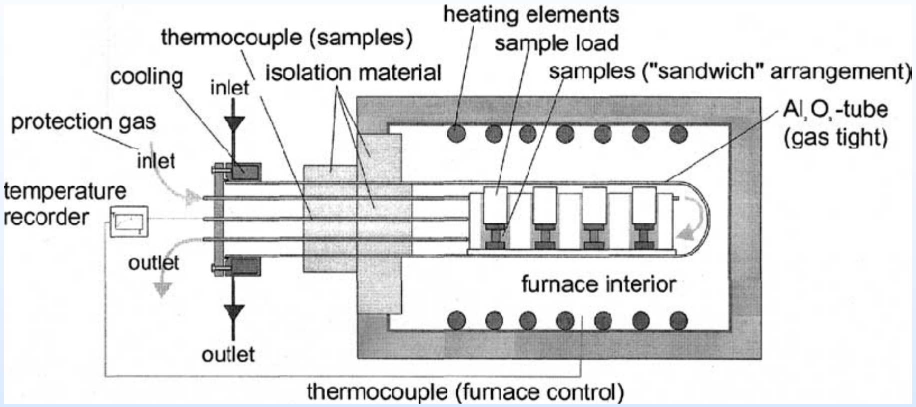

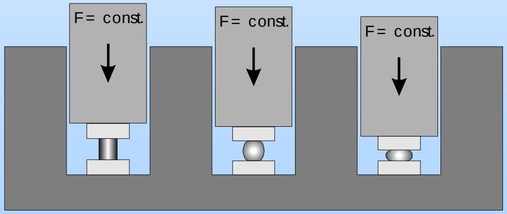

Melt Corrosion

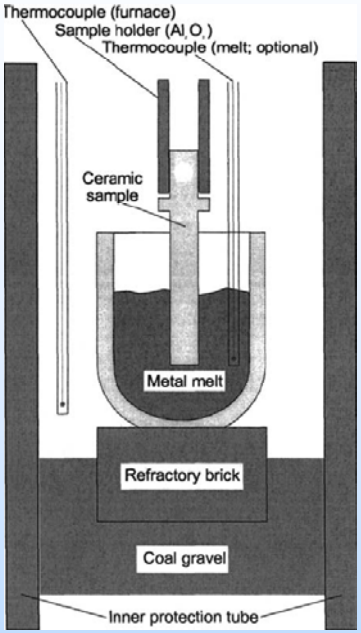

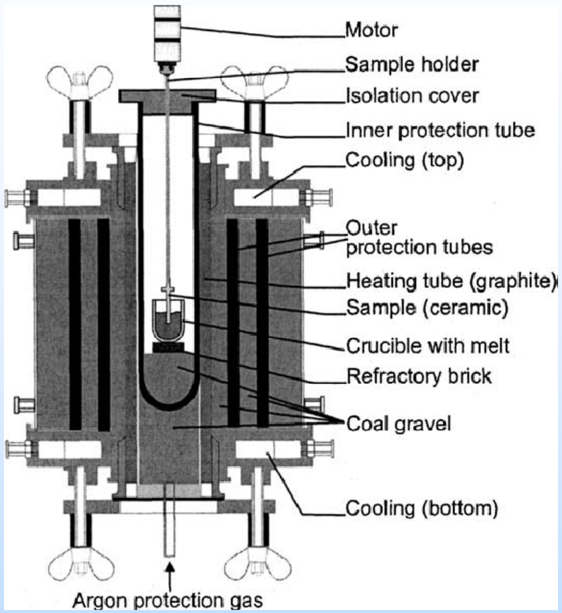

Steel HS 6-5-2
Phase Composition as a Function of Temperature

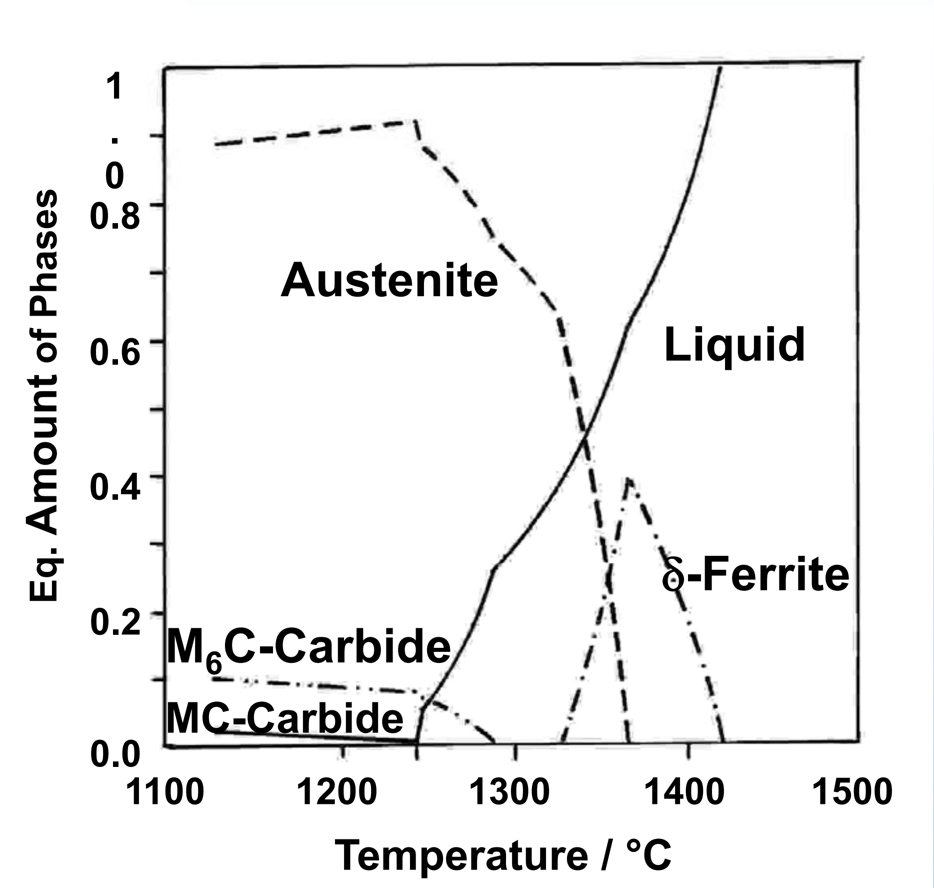

°C	Literature	Calculation
$T_{Solidus}$	1220	1234
$T_{Liquidus}$	1427	1427
Δ T	207	193

Stahl	C	Si	Mn	S	Cr	Mo	Ni	V	Cu	Al	Ti	N	W
HS 6-5-2	0.86	0.25	0.29	0.003	4.05	**4.59**	0.35	**1.8**	0.07	<0.01	<0.01	0.017	**6.15**

Stahl HS 6-5-2 / 1330°C
Phase Composition as a Function of Oxygen Partial Pressure

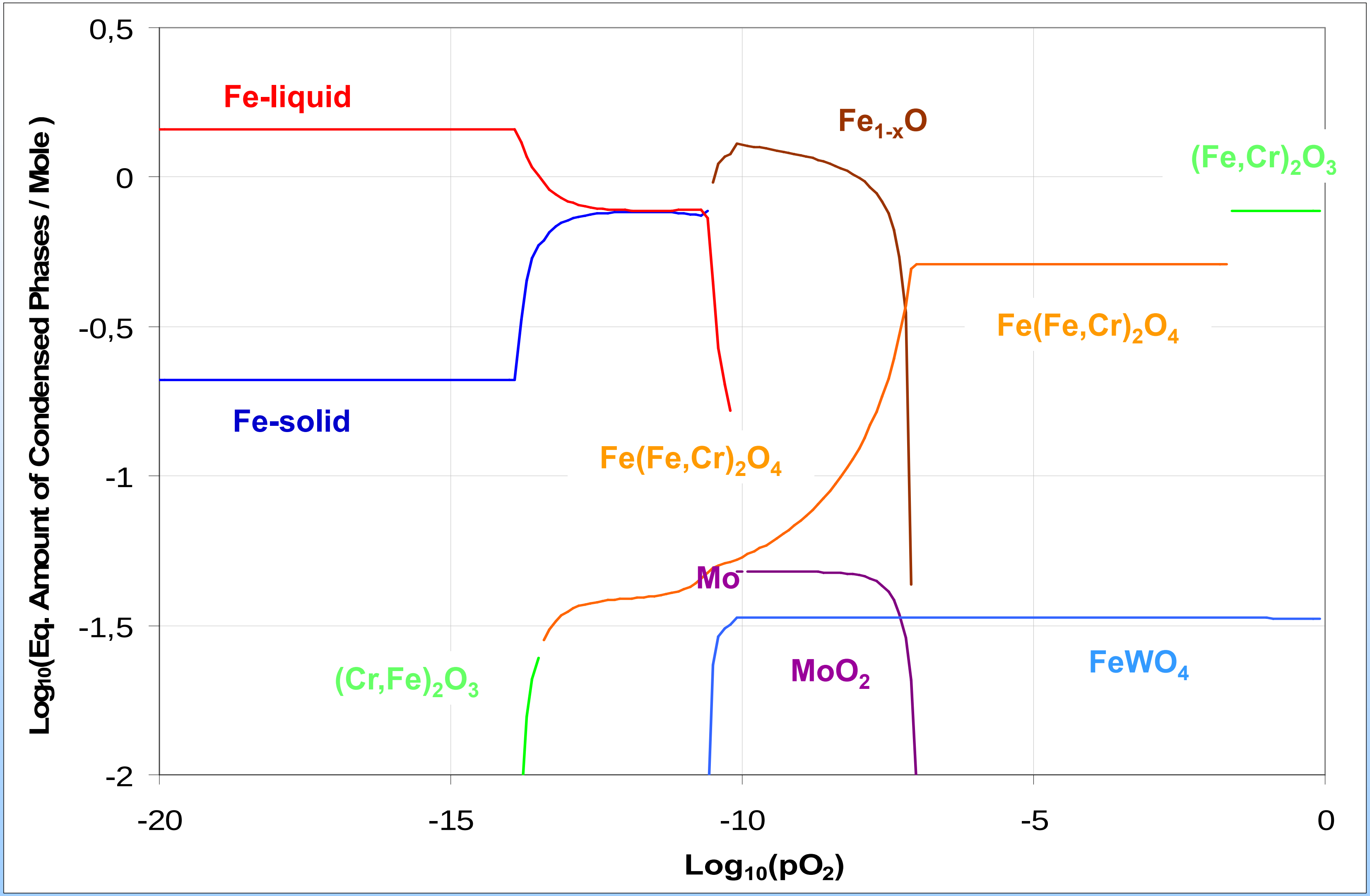

Thermochemical Calculations
Applied to High Temperature Corrosion
of Ceramic and Refractory Materials

RWTH AACHEN UNIVERSITY

Contact Corrosion of $CaZrO_3$ – Steel HS 6-5-2 at 1330°C

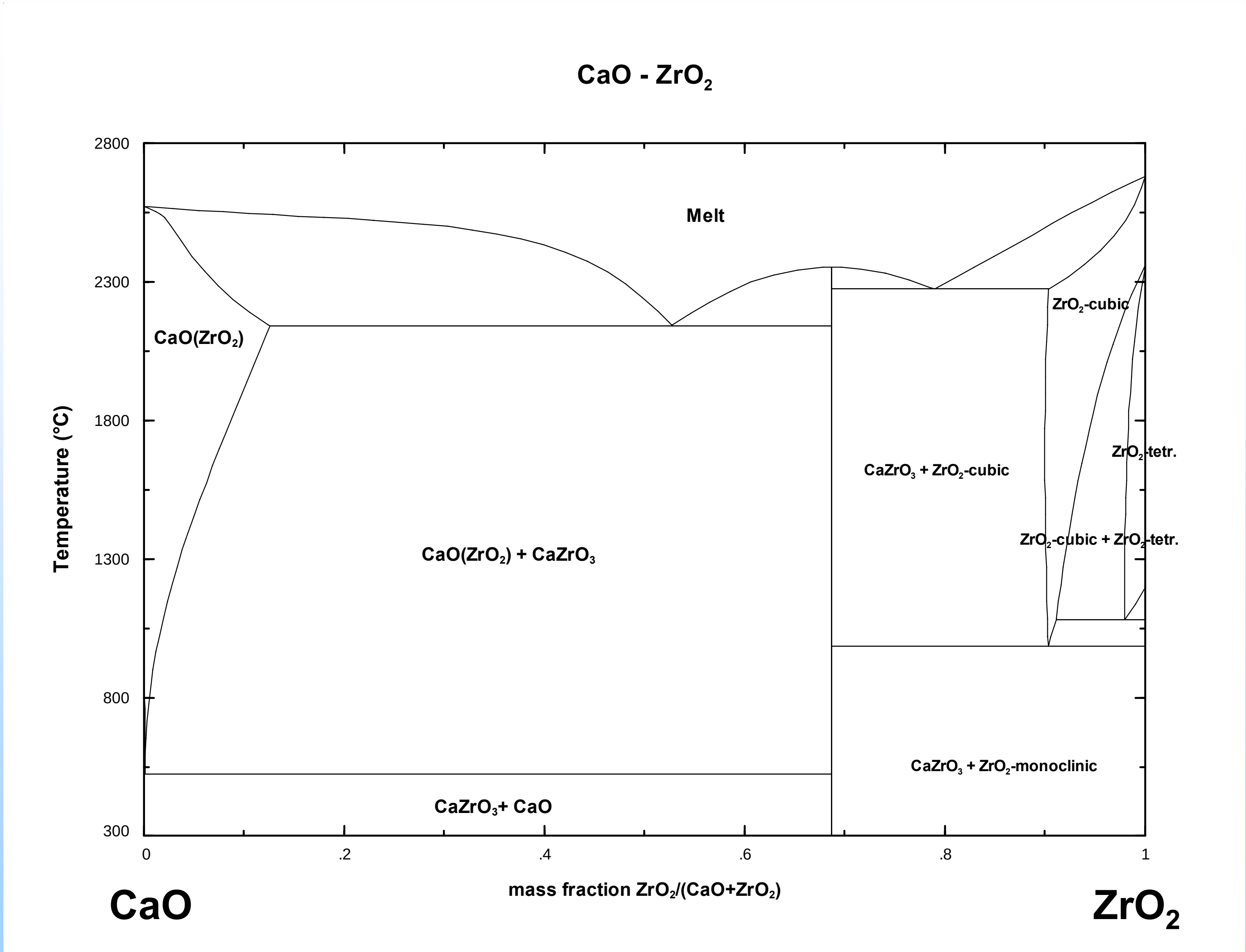

Contact Corrosion of $CaZrO_3$ – Steel HS 6-5-2 at 1330°C
Phase Stabilities as a Function of Oxygen Partial Pressure

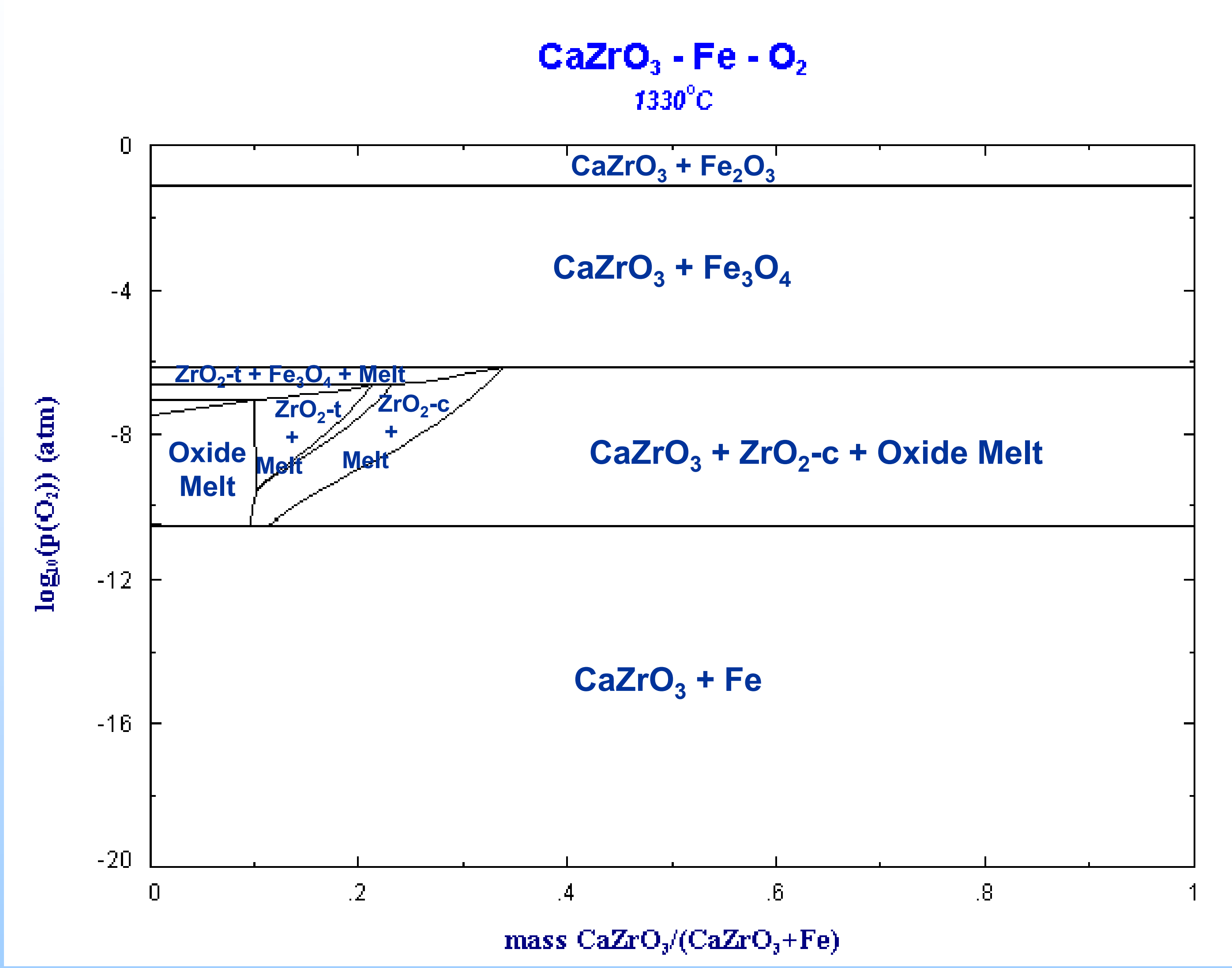

System Fe – $CaZrO_3$ – O_2 / 1330 °C

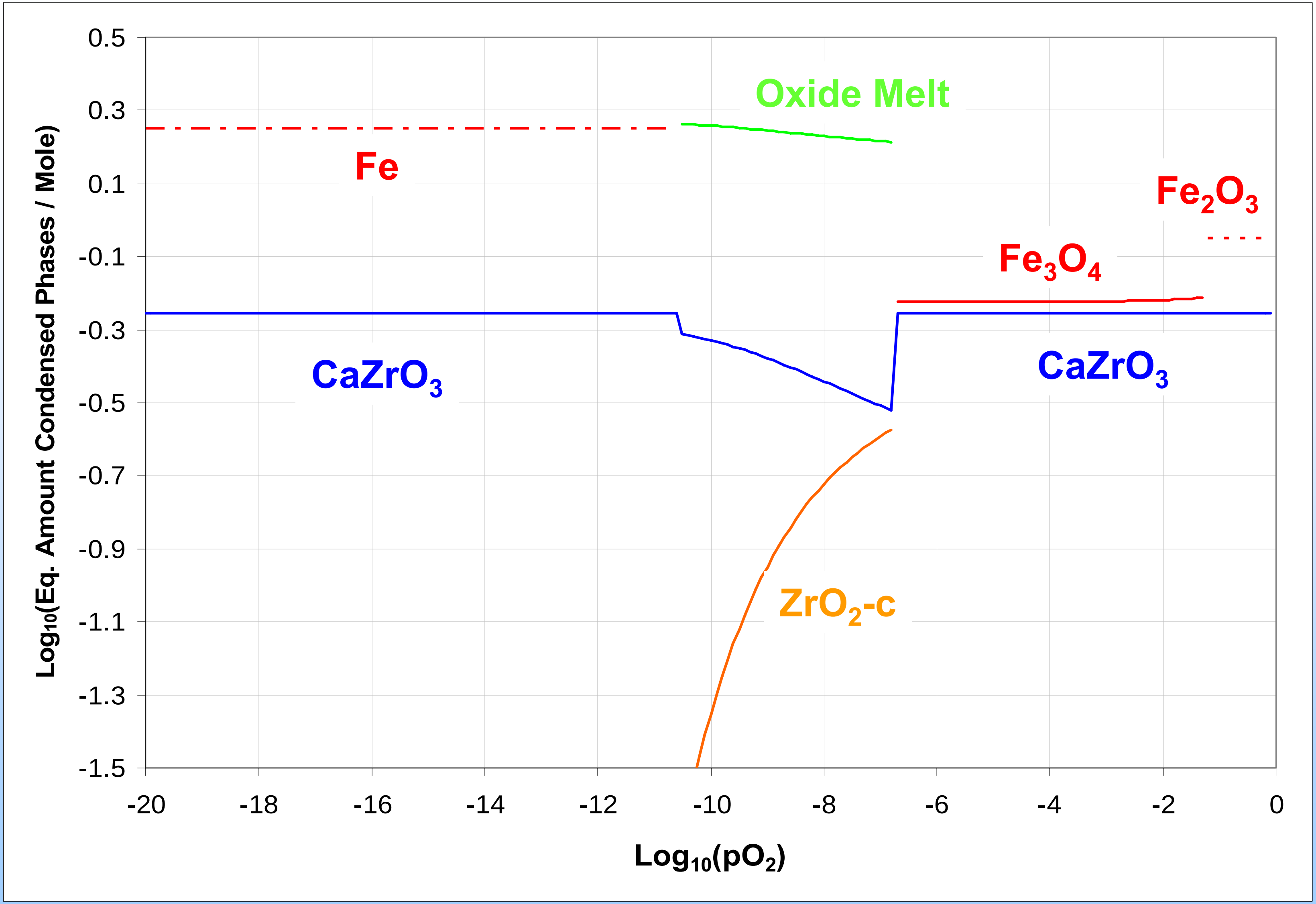

System Fe – $CaZrO_3$ – O_2 / 1330°C
Composition of Oxide Melt

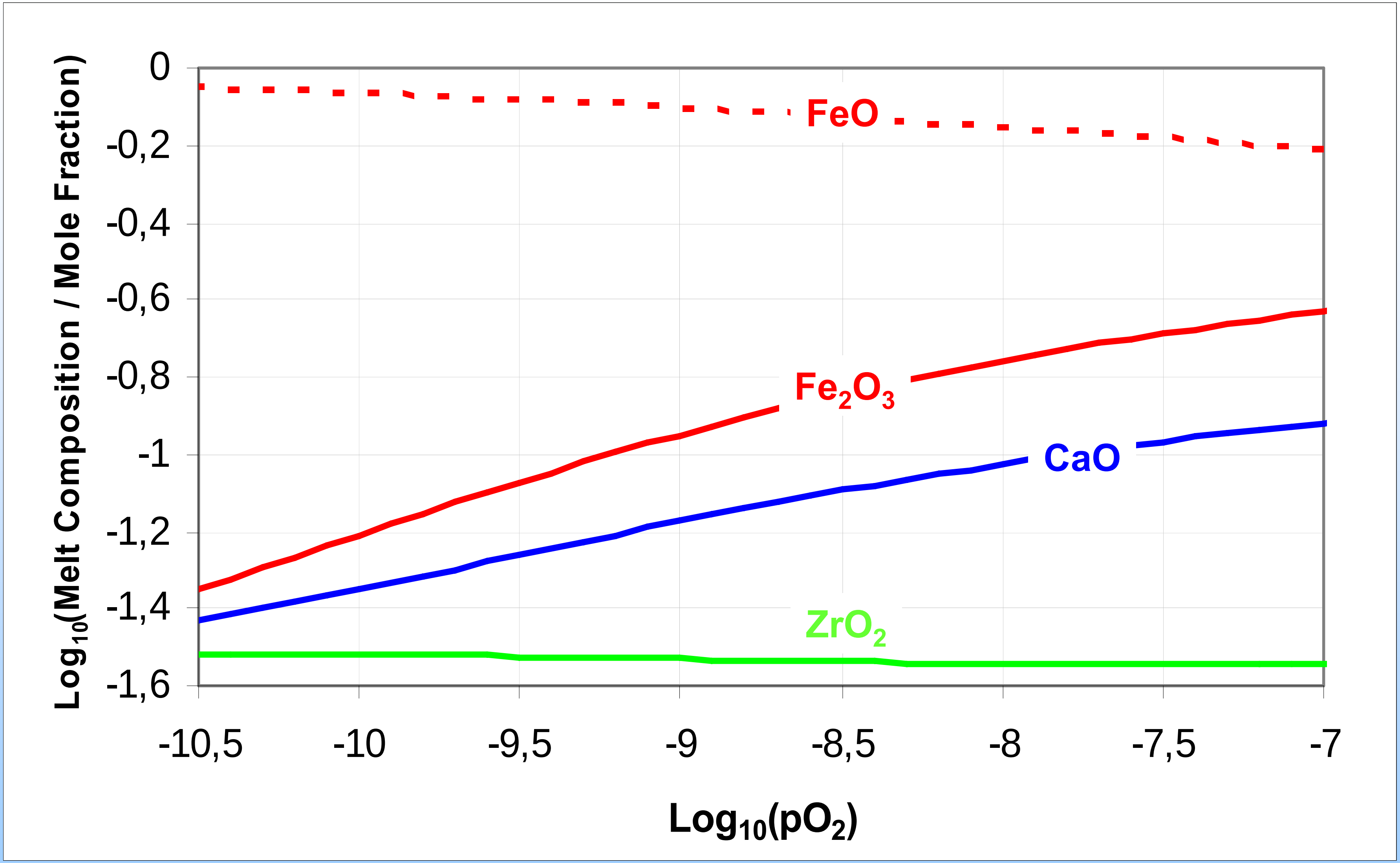

Contact Corrosion of $CaZrO_3$ – Steel HS 6-5-2 at 1330°C
Phase Reactions with the Alloying Elements of Steel HS 6-5-2

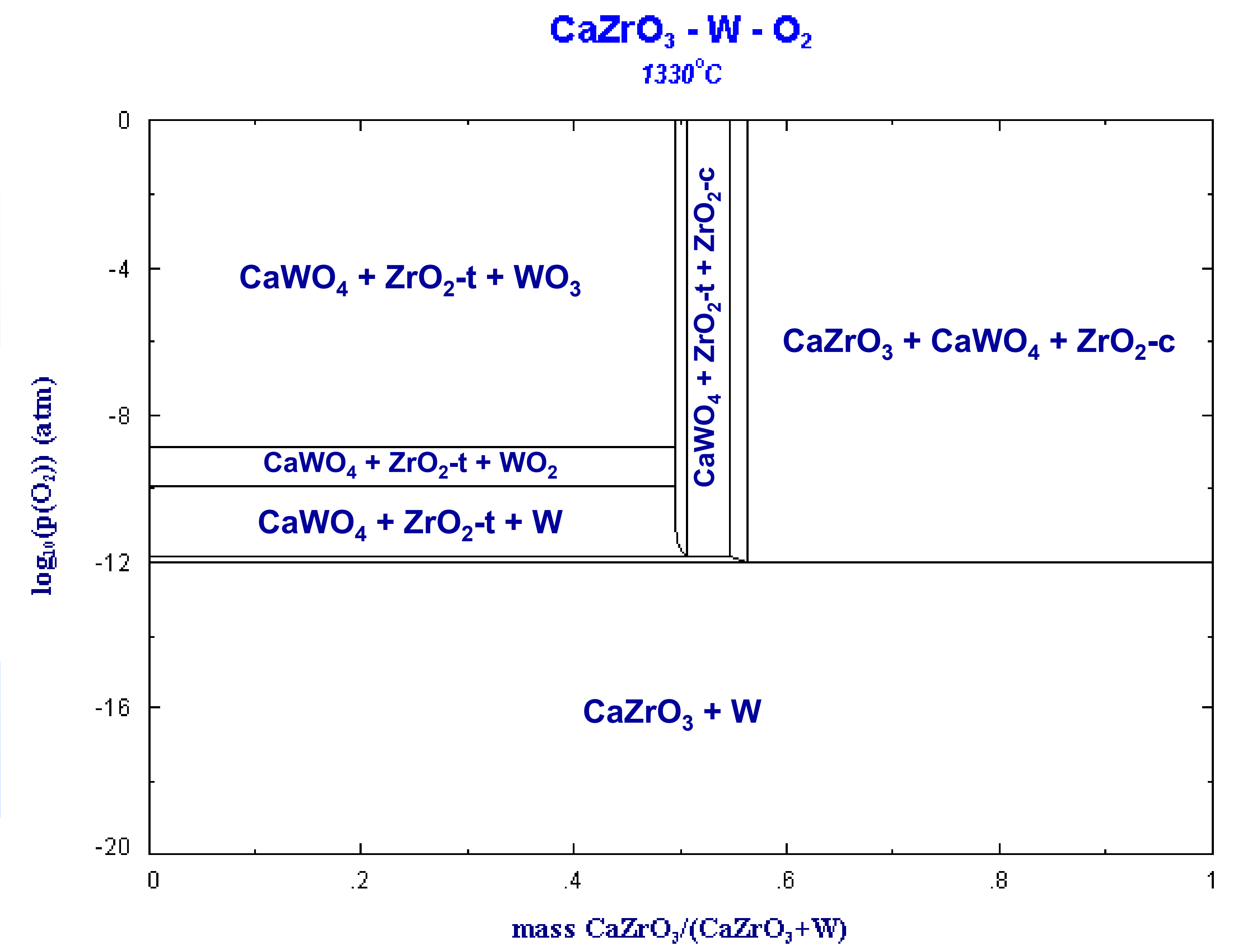

Contact Corrosion of $CaZrO_3$ – Steel HS 6-5-2 at 1330°C
Phase Reactions with the Alloying Elements of Steel HS 6-5-2

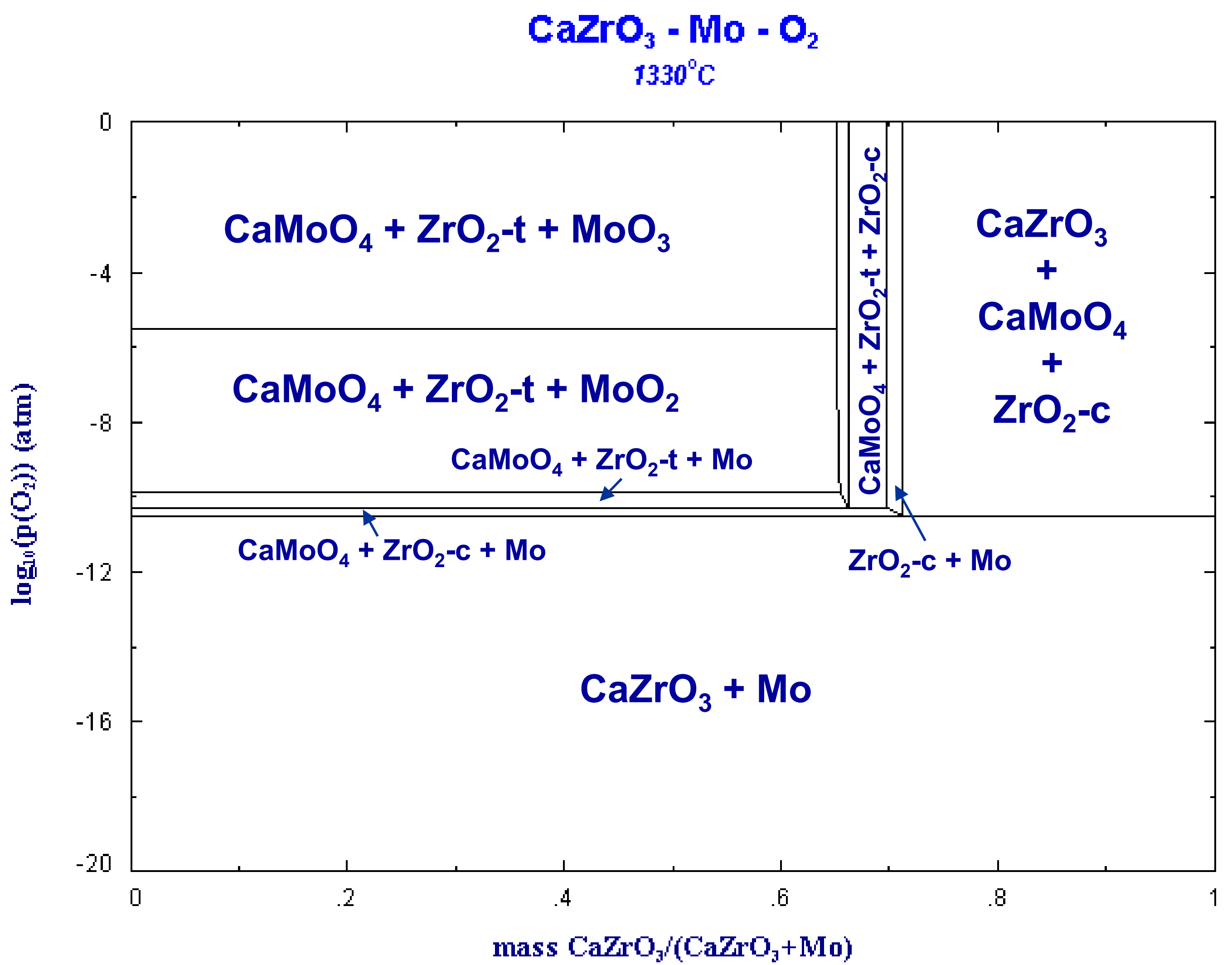

Contact Corrosion of $CaZrO_3$ – Steel HS 6-5-2 at 1330°C
Phase Reactions with the Alloying Elements of Steel HS 6-5-2

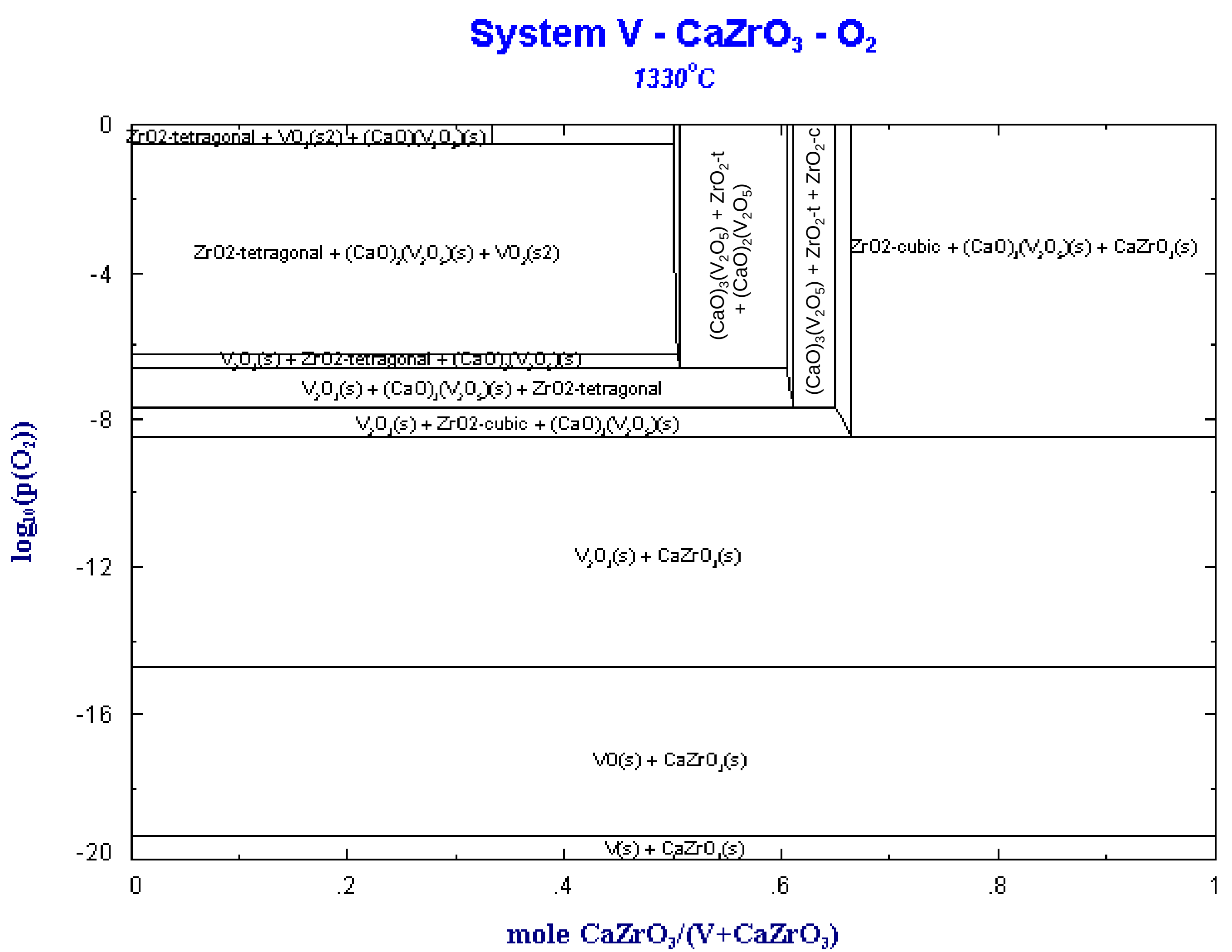

Thermochemical Calculations
Applied to High Temperature Corrosion
of Ceramic and Refractory Materials

RWTH AACHEN UNIVERSITY

Contact Corrosion of $CaZrO_3$ – Steel HS 6-5-2 at 1330°C
Phase Reactions as Function of Oxygen Partial Pressure

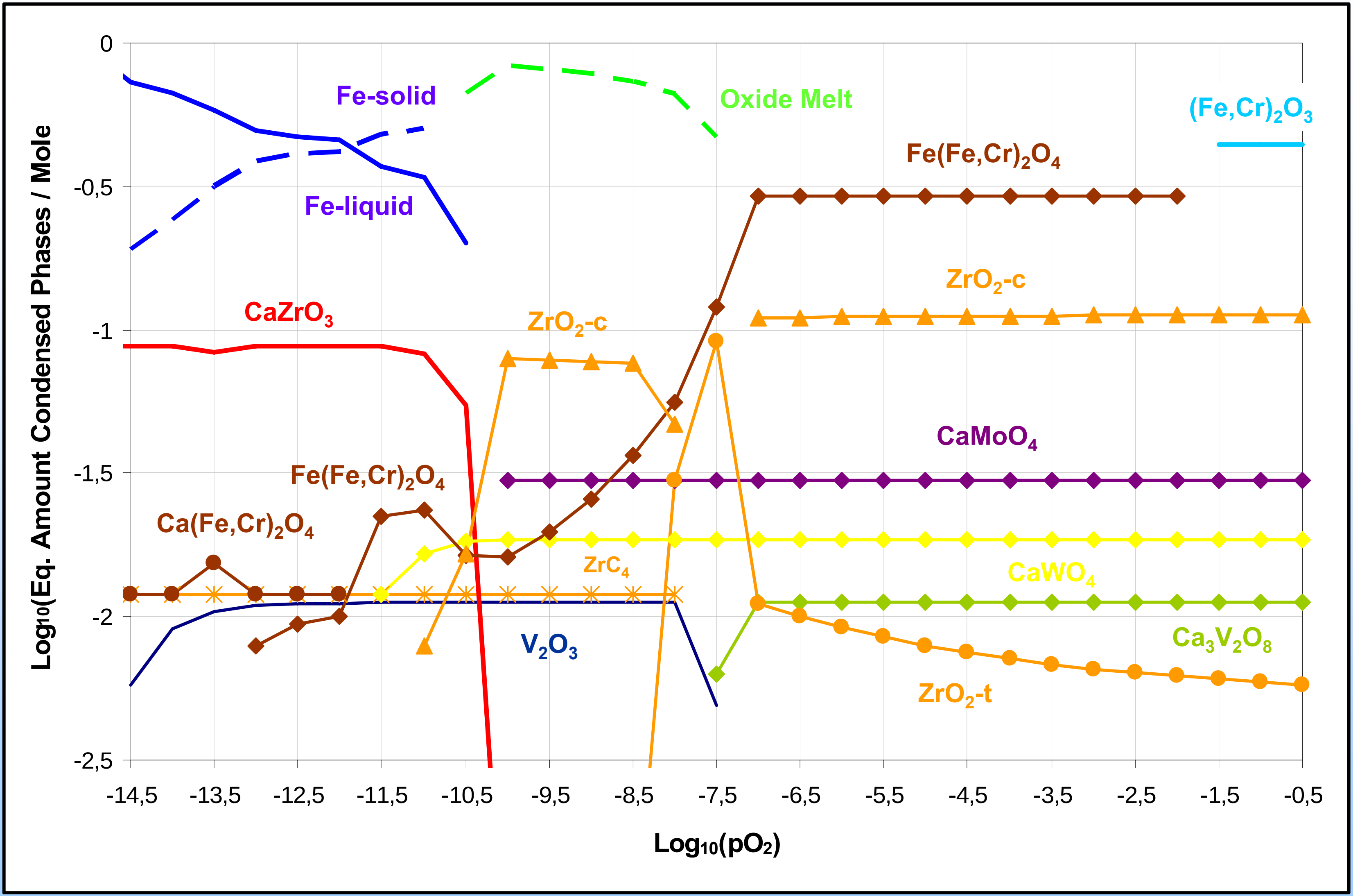

Contact Corrosion of $CaZrO_3$ – Steel HS 6-5-2 at 1330°C
Composition of Fe-Liquid

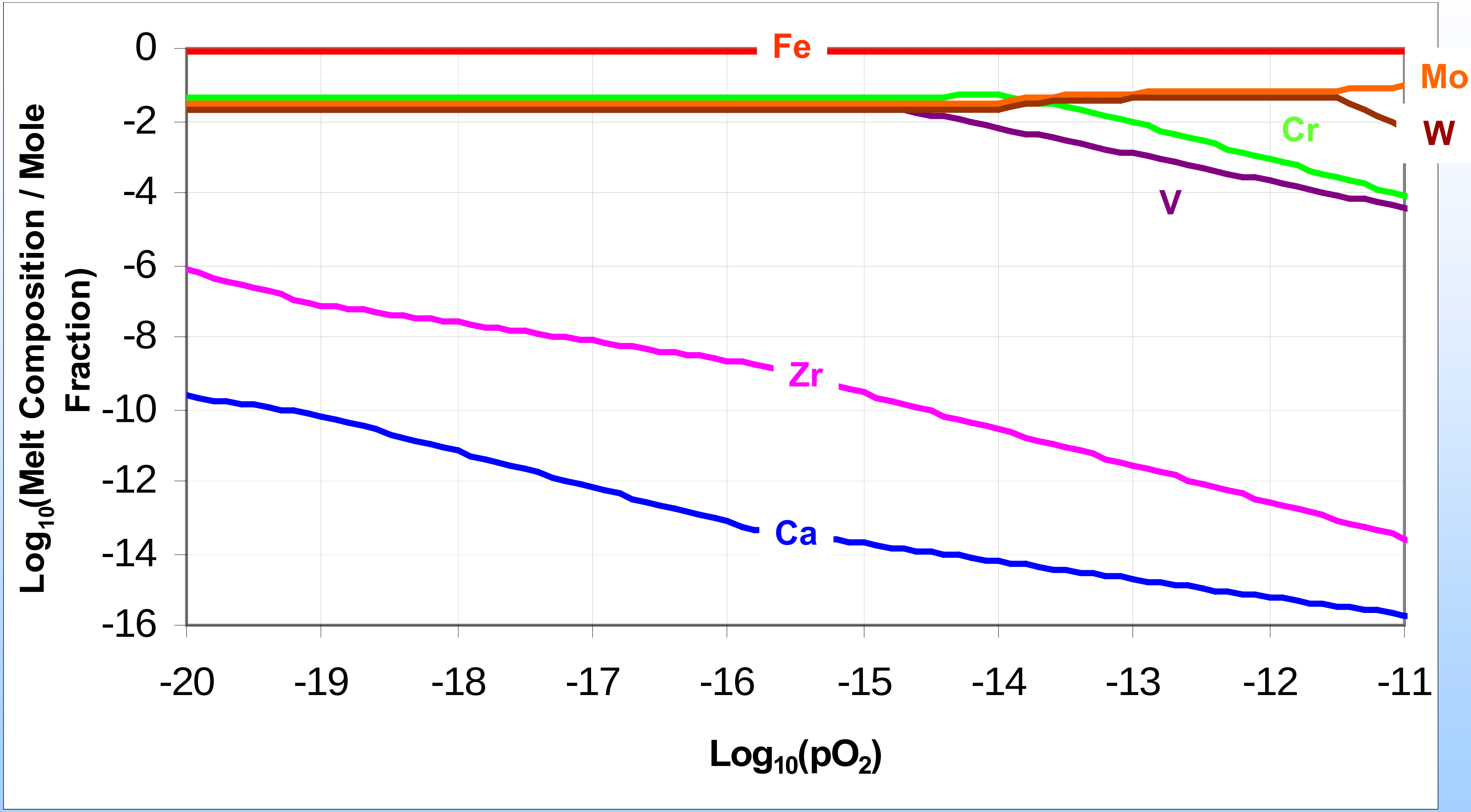

Contact Corrosion of $CaZrO_3$ – Steel HS 6-5-2 at 1330°C
Composition of Oxide Melt

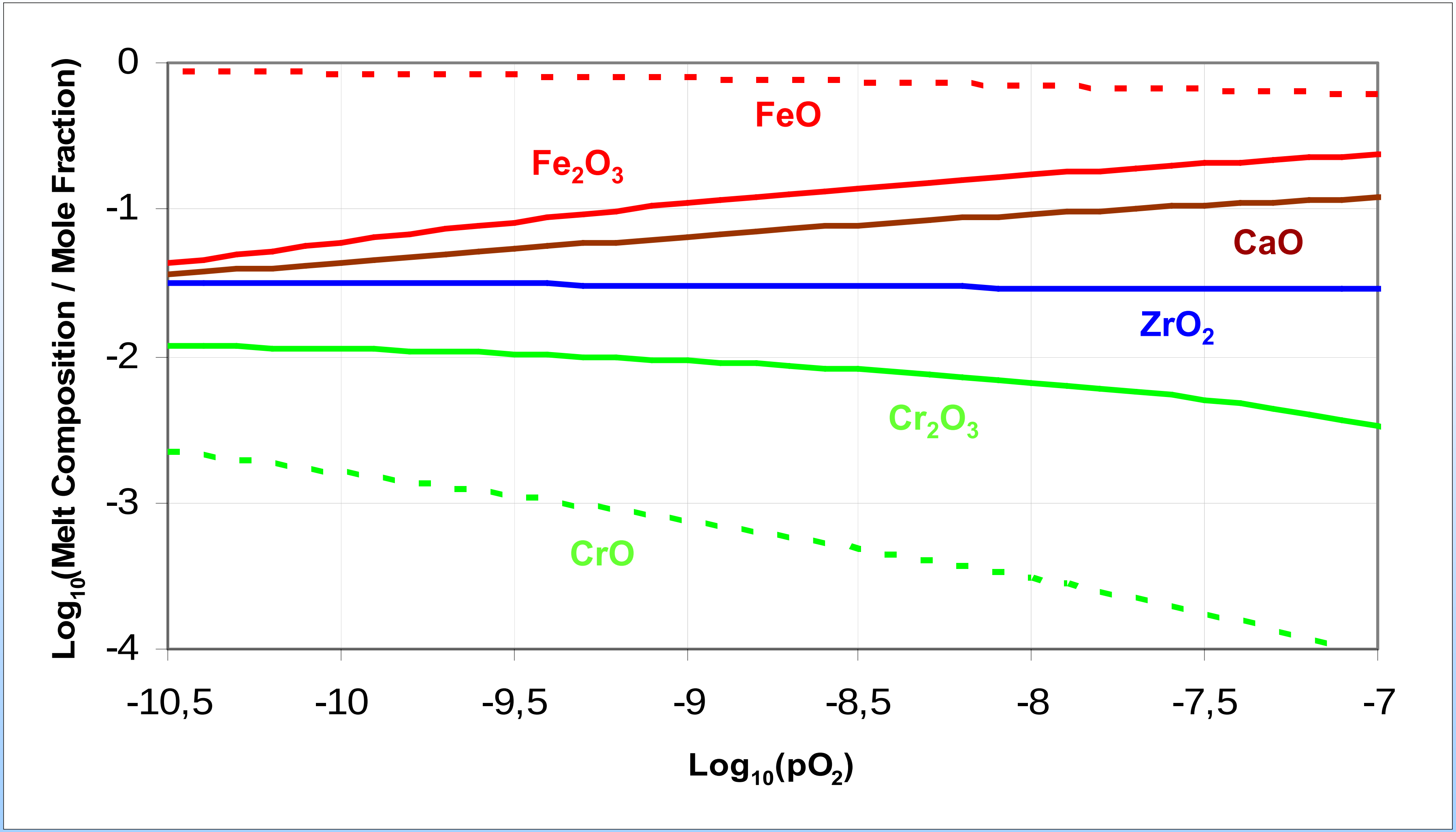

Contact Corrosion of $CaZrO_3$ – Steel HS 6-5-2 at 1330°C
Phase Reactions between $CaZrO_3$ and the Oxide Scale of Steel HS 6-5-2

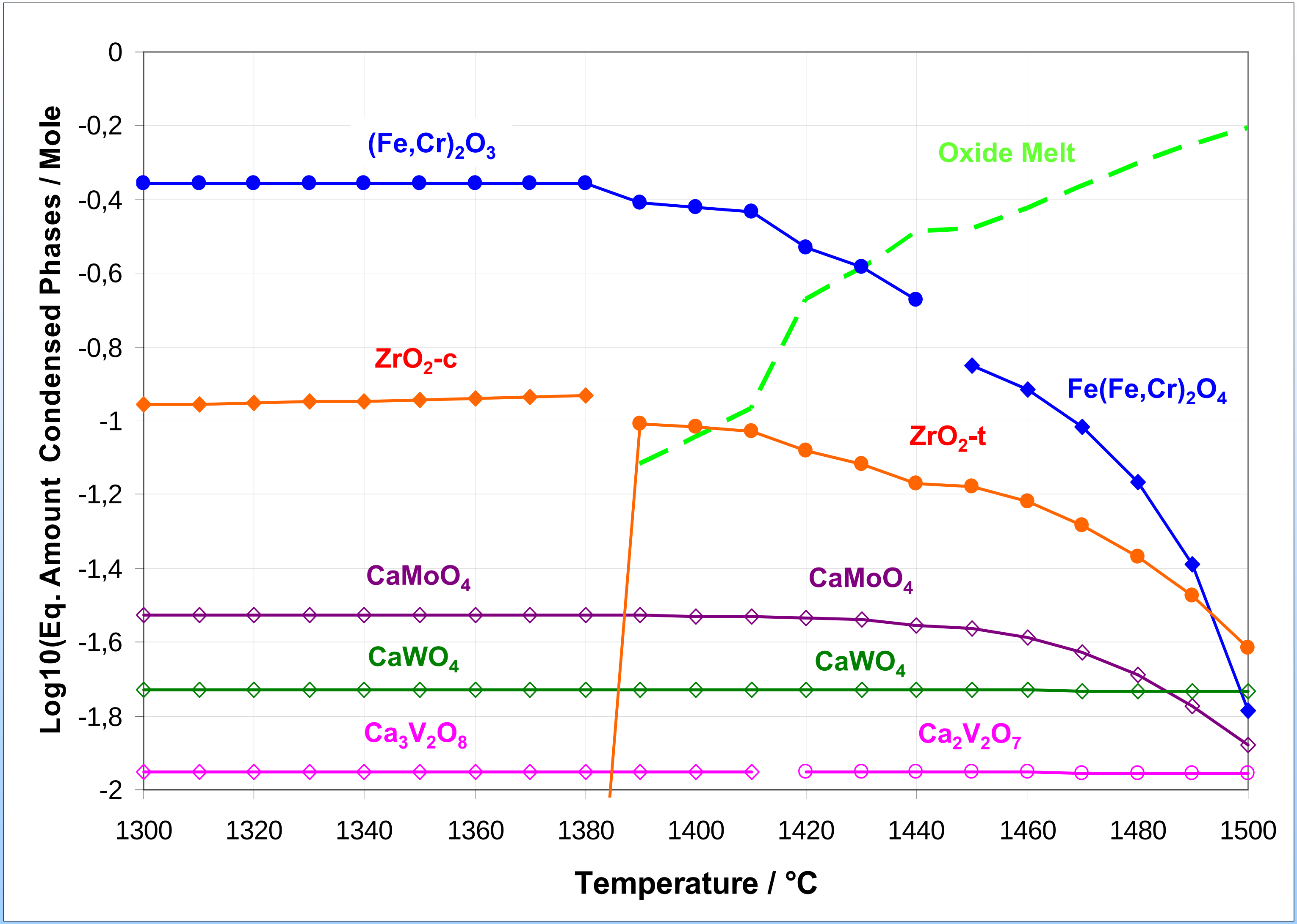

Contact Corrosion of $CaZrO_3$ – Steel HS 6-5-2 at 1330°C (2h / air)

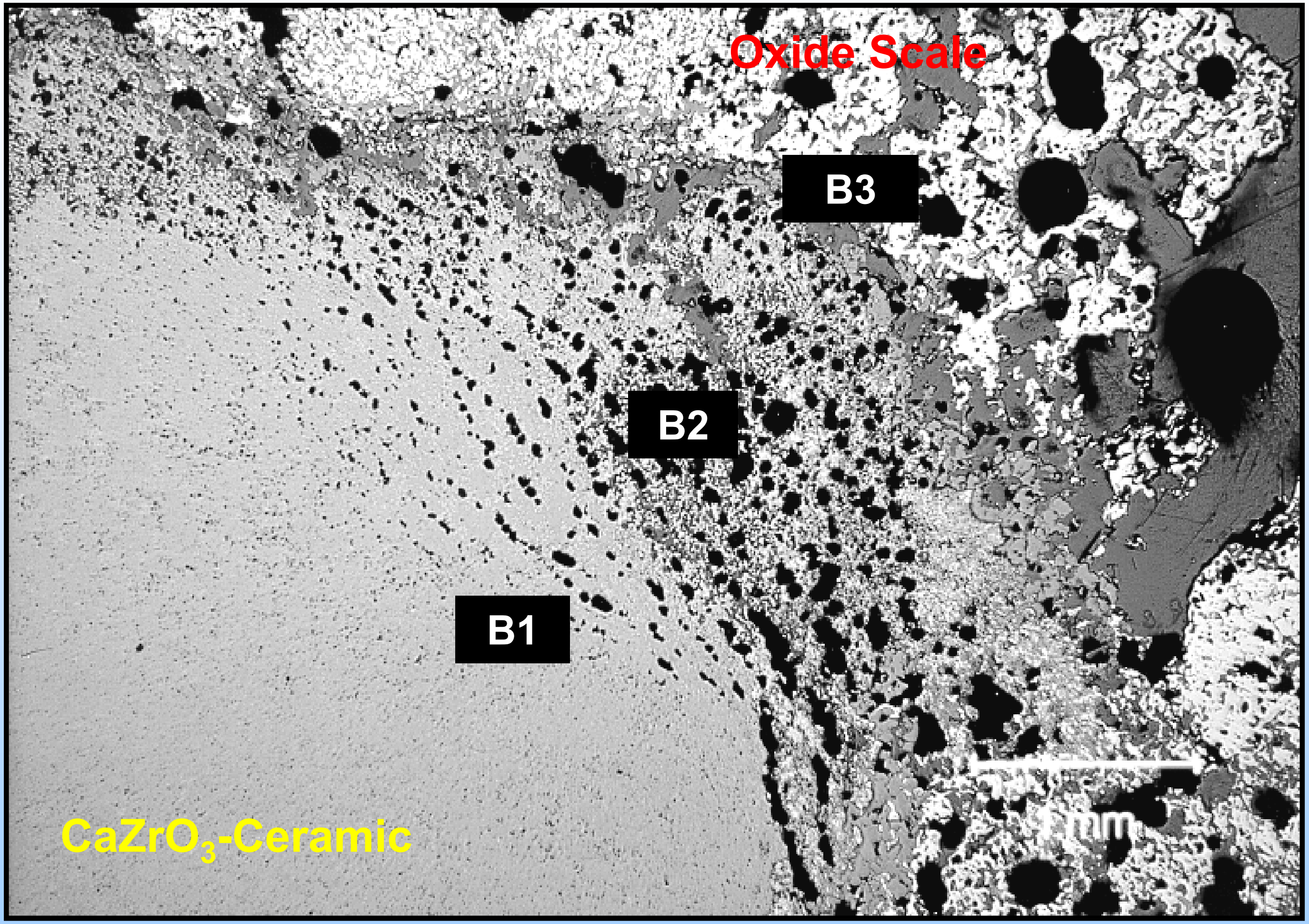

Contact Corrosion of $CaZrO_3$ – Steel HS 6-5-2 at 1330°C (2h / air)

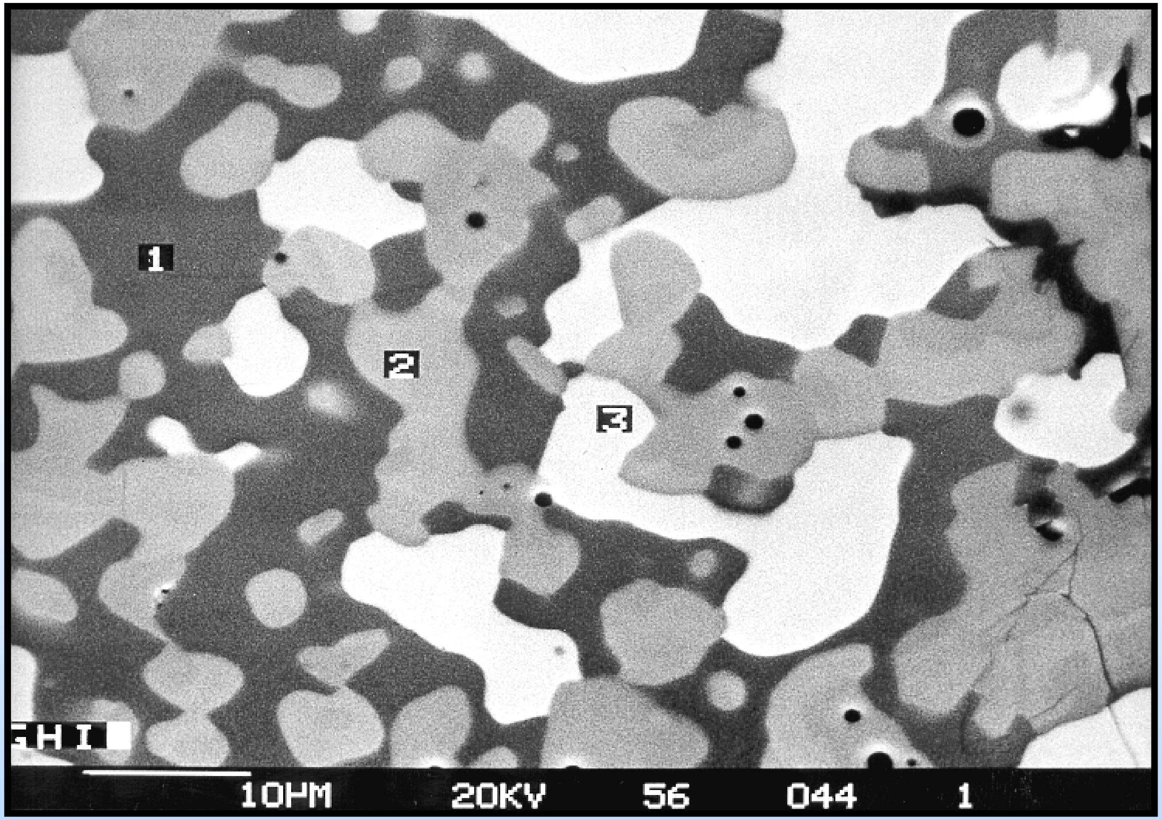

Area B1:

- dense microstructure
- pores formation in $CaZrO_3$ grains
- infiltration along the grain boundaries [1]
- dissolution of the $CaZrO_3$ grains [2] → enrichment of Ca + Zr in the infiltrating grain boundary phase [1]
- precipitation of ZrO_2 solid solution [3]

	[At.-%]	Ca	Zr	Fe	W	V
1	infiltrating grain boundary phase	38.8	27.1	28.6	1.7	3.6
2	$CaZrO_3$	50.0	43.1	5.2	1.7	-
3	ZrO_2-solid sol.	19.9	74.8	5.3	-	-

Contact Corrosion of $CaZrO_3$ – Steel HS 6-5-2 at 1330°C (2h / air)

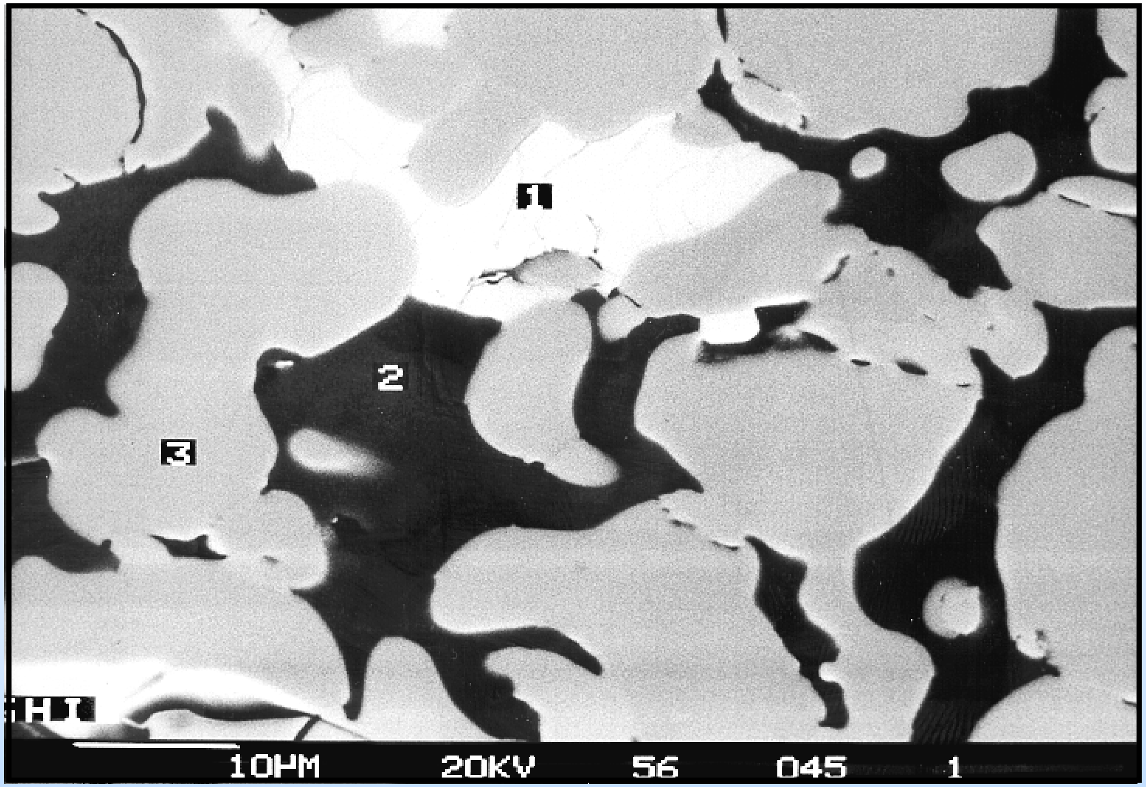

Area B2:

- advanced decomposition of microstructure
- no $CaZrO_3$
- infiltration along grain boundaries [2]
- new phases formed by reaction of solved Ca with the alloying elements → $CaMoO_4$ (Powellite) – $CaWO_4$ (Scheelite)–solid sol. [1]
- formation of ZrO_2 – solid solutions [3]

	[At.-%]	Ca	Zr	Mo	Fe	W	V	Si
1	$Ca(Mo,W)O_4$ – solid sol.	47.7	-	33.1	-	19.3	-	-
2	infiltrating grain boundary phase	36.4	21.6	-	30.1	-	5.2	6.8
3	ZrO_2-solid sol.	16.8	75.1	-	8.1	-	-	-

Contact Corrosion of CaZrO3 – Steel HS 6-5-2 at 1330°C (2h / air)

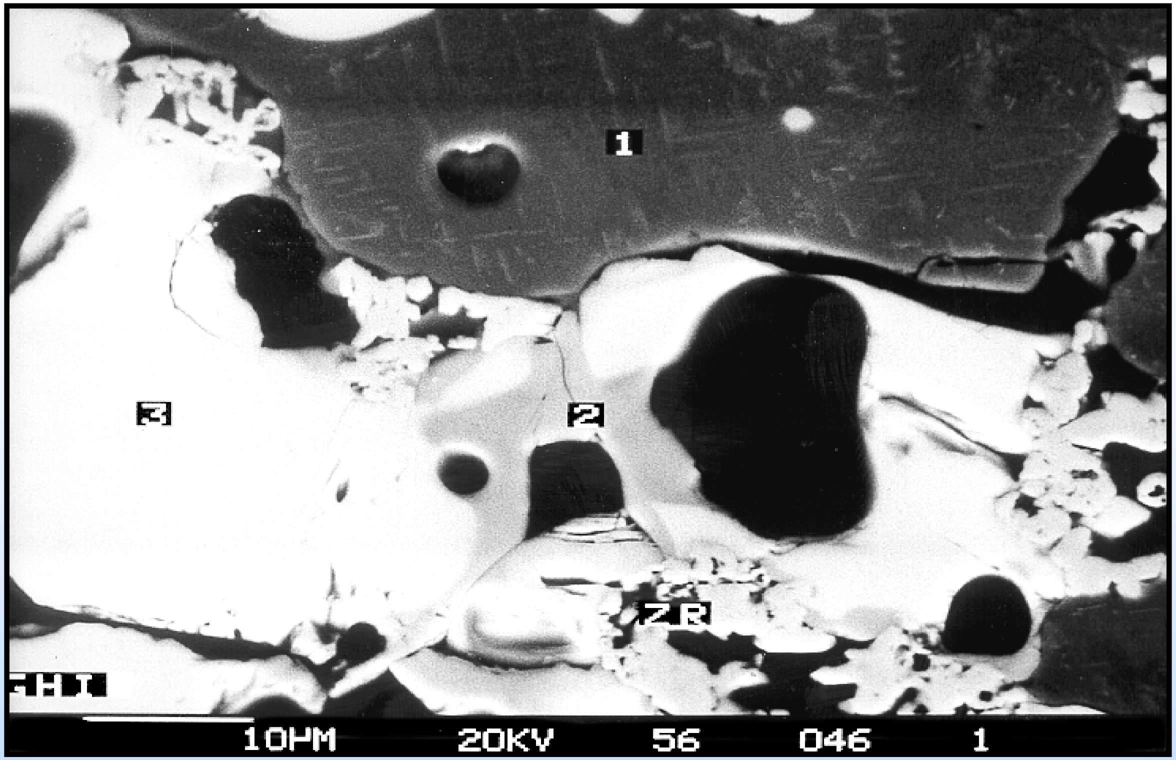

Area B3:

- porous oxide scale with ZrO_2-grains [Zr] / no solid solution
- (Fe,Cr)-Oxide – solid sol. [1]
- Formation of $CaMoO_4$ (Powellite) – $CaWO_4$ (Scheelite) – $FeWO_4$ (Ferberite) solid solutions [2], [3]

	[At.-%]	Ca	Zr	Mo	Fe	W	Cr
1	$(Fe,Cr)_2O_3$		4.5	-	85.4	-	10.2
2	$Ca(Mo,W)O_4$ – solid solution I	48.7	-	41.7		9.7	-
3	$Ca(Mo,W)O_4$ – solid solution II	48.2	-	31.5	-	20.2	-

Contact Corrosion of $CaZrO_3$ – Steel HS 6-5-2 at 1330°C
Phase Reactions as Function of Oxygen Partial Pressure

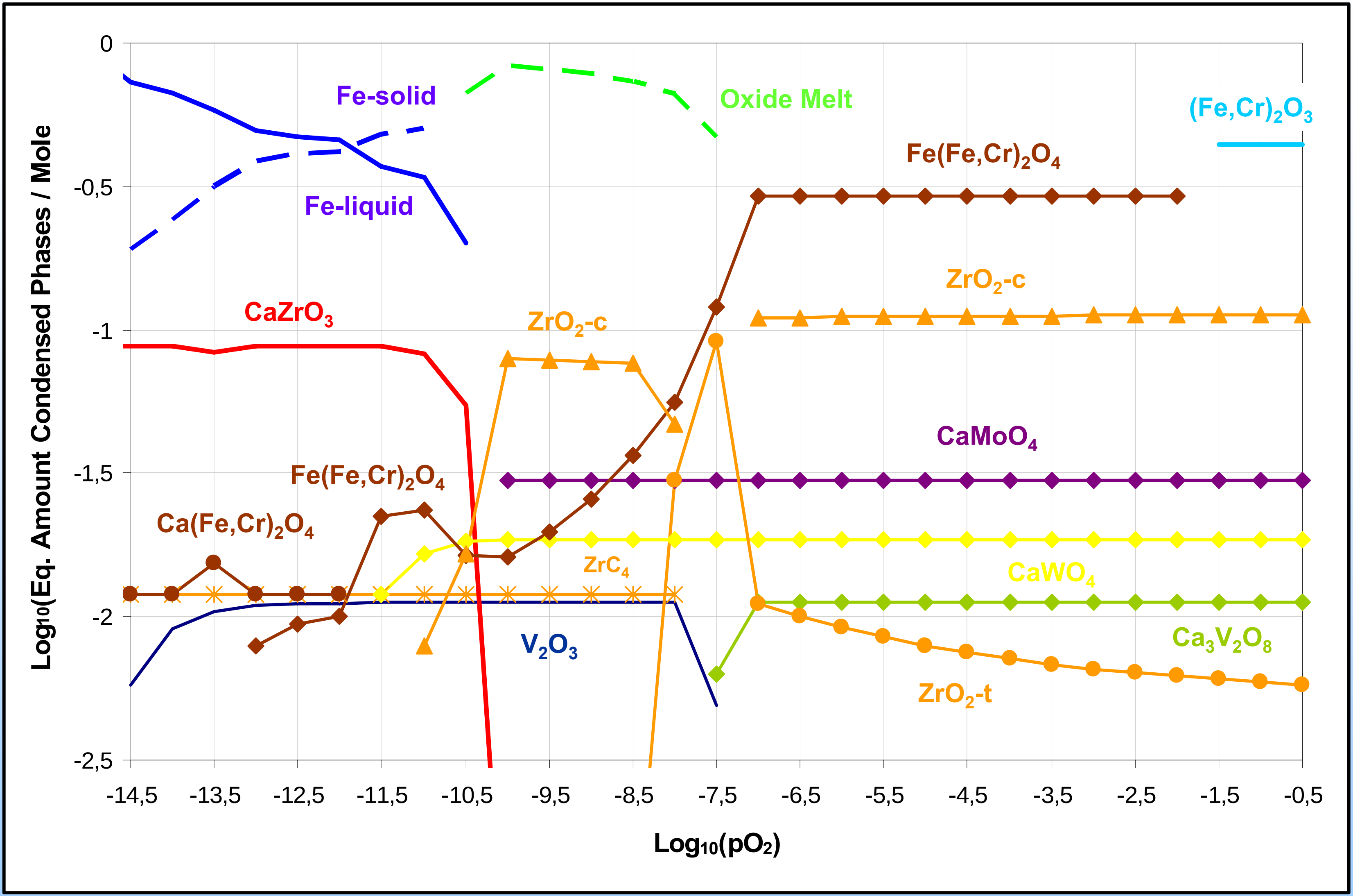

Contact Corrosion of $CaZrO_3$ – Steel HS 6-5-2 at 1330°C (Ar-5%H_2)

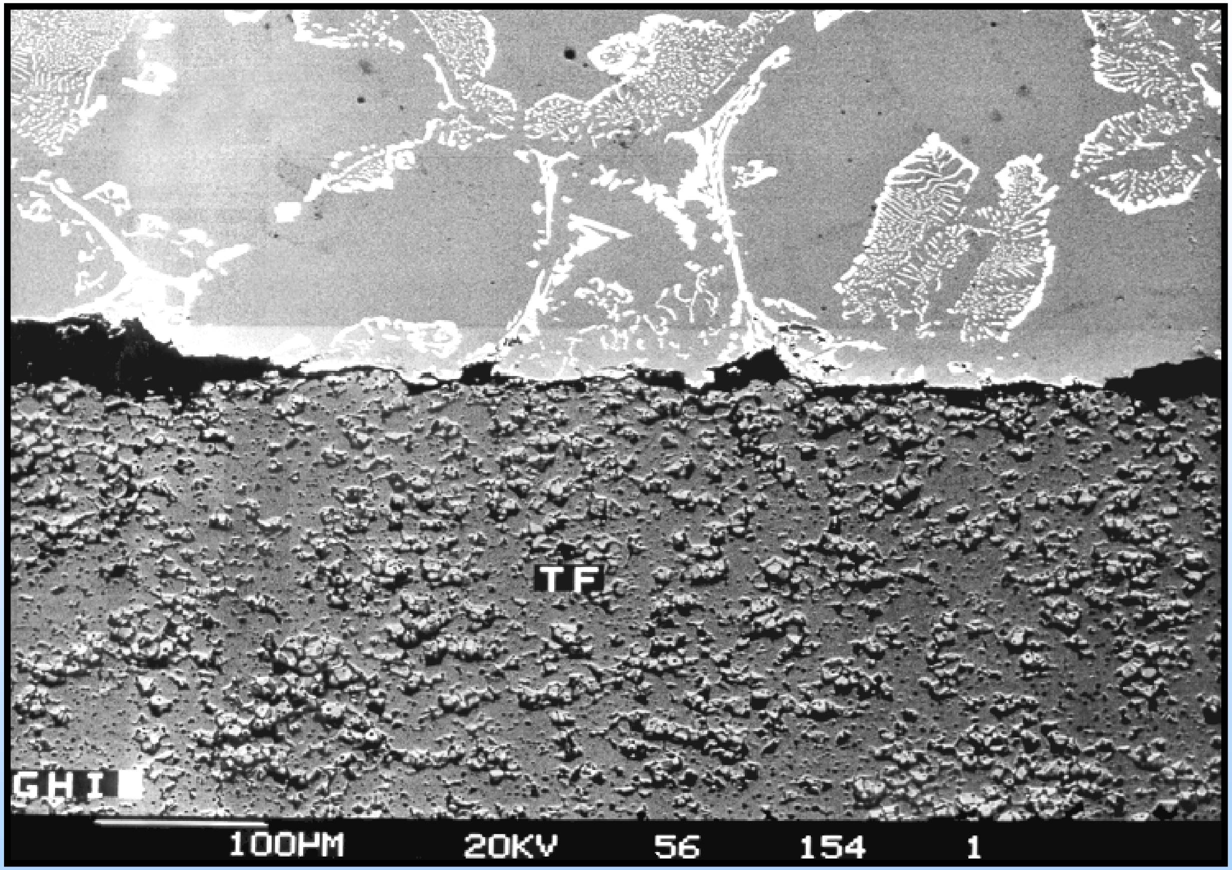

Melt Corrosion $CaZrO_3$ – Steel HS 6-5-2
1470 °C / Ar 4.6 / 1h

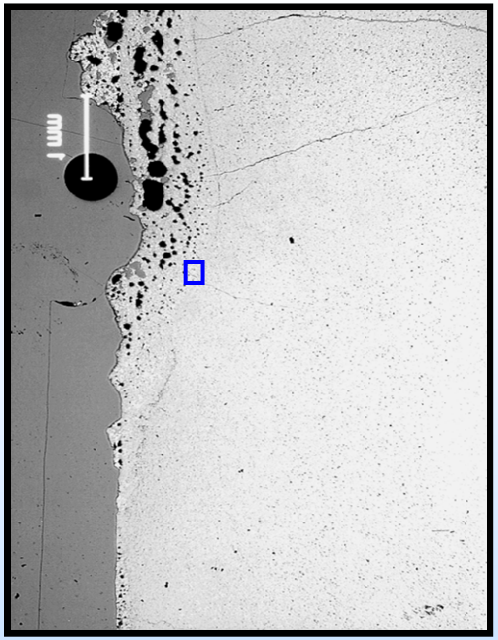

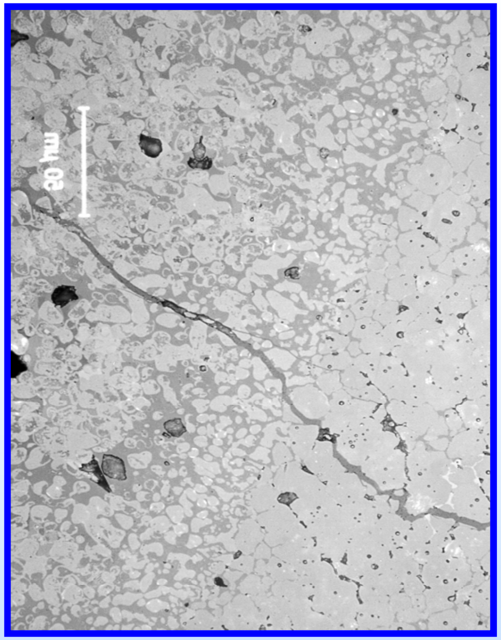

Area of Melt Surface

- dissolution of the ceramic material
- formation of a high porous layer
- formation of cracks

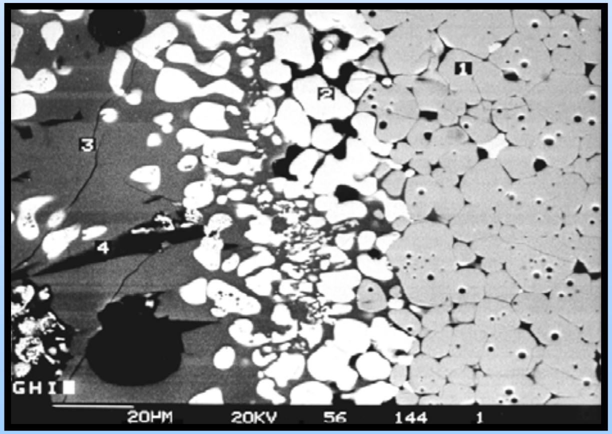

Contact
Slag - Ceramic

Corrosion Process:

-Infiltration along Grain Boundaries
-Dissolution of the Ceramic Material
-CaO solution in the infiltrating Grain Boundary Phase
-Precipitation of ZrO_2-Soild Solution
-Pores- and Crack-Formation

Zircon based Refractory Materials

Excellent Thermphysical Properties:

- low thermal expansion
- low thermal conductivity
- good corrosion resistance against glass melts, slags and liquid metal alloys

Applications as Refractory Materials:

- construction material in glass tanks, in iron and steel production, in energy technology
- moulds and cores in precision investment casting
- protective coatings of steel-moulding tools

→ Extremely differing information concerning the thermal stability of $ZrSiO_4$ and the temperature and the kinetics of the solid state dissociation $ZrSiO_4 \Leftrightarrow ZrO_2 + SiO_2$

→ Substantial information for predicting service life and long-time behaviour of zircon based refractories

➡ temperature, reaction mechanism, kinetics of zircon-decomposition f(impurities, grain size, grainsize distribution, …)

Literature Review : Thermal Decomposition of $ZrSiO_4$

$\Delta T_{diss.} = 517\ K$

Author	Year	Decomposition of $ZrSiO_4$	Temperature
Washburn & Libman	1920	congruent melting	2550°C
Zhirnowa	1934	congruent melting	2430°C
Geller & Lang	1945	incongruent melting	**1775°C**
Curtis & Sowman	1953	solid state dissociation	1540°C
Toropov & Galakhov	1956	solid state dissociation	1540ºC
Cocco & Schromek	1958	incongruent melting	1720°C
Rosén & Muan	1965	solid state dissociation	1600–1650 °C
Butterman & Foster	1967	solid state dissociation	1676°C
Jones, Kimura & Muan	1967	solid state dissociation	1675 ± 10 °C
Wecht	1972	solid state dissociation	1640 °C
Anseau, Biloque & Fierens	1976	solid state dissociation	>1525-1634°C
Fischer, Janke & Schulenburg	1976	solid state dissociation	1650-1680 °C
Klute & Woermann	1982	solid state dissociation	1681 ± 5 °C
Kanno	1989	solid state dissociation	1650-1700°C
Pavlik & Holland	2001	solid state dissociation	**1258 °C**
Levin	2001	solid state dissociation	1550 °C
O´Neill	2003	solid state dissociation	1667 °C

Literature Review : Phase Relationships in the System ZrO_2-SiO_2 - System

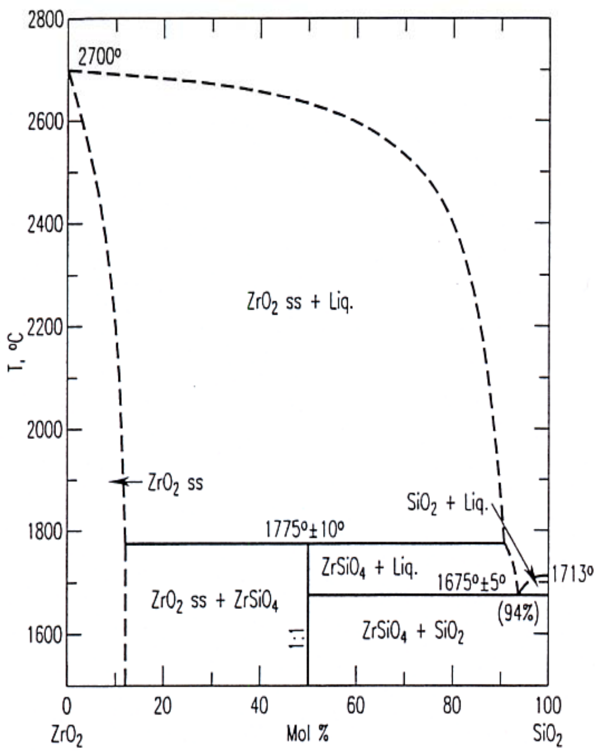

Geller & Lang (1959)

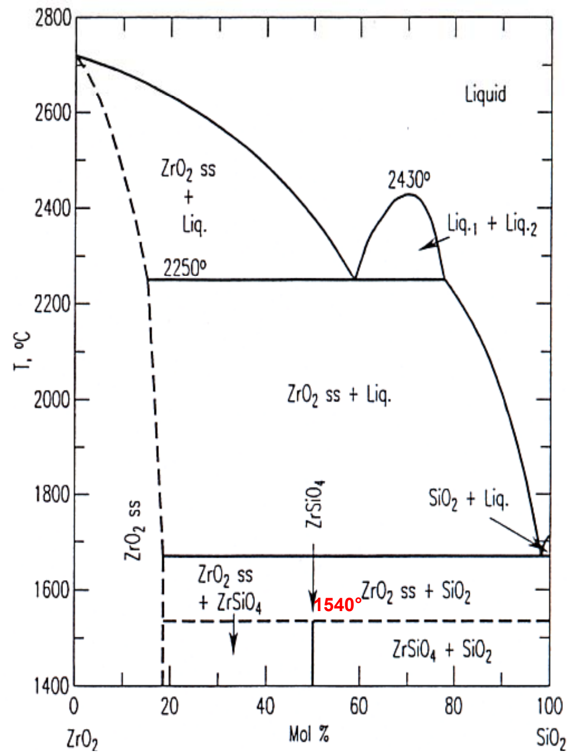

Toropov & Galakhov (1956)

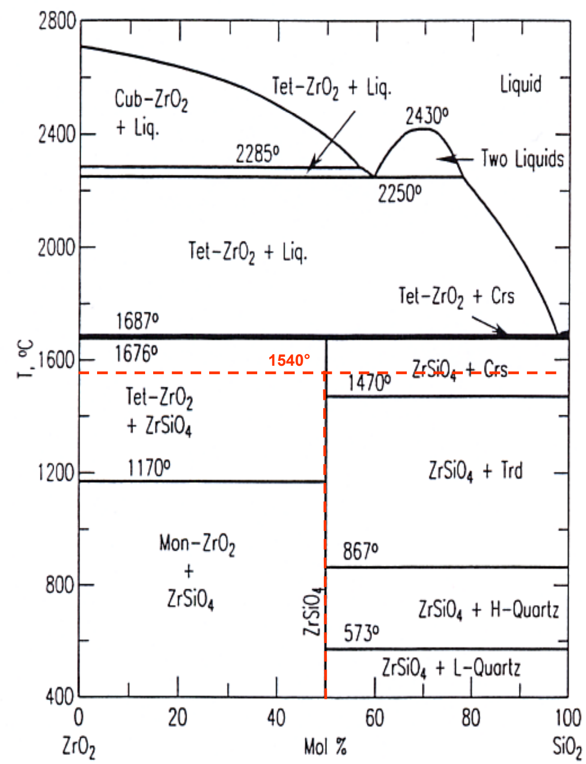

Butterman & Foster (1967)

Curtis & Sowman (1953)

$\Delta T_{diss.} = 136$ K

$ZrSiO_4$ Decomposition Mechanism - Single Crystal Experiments

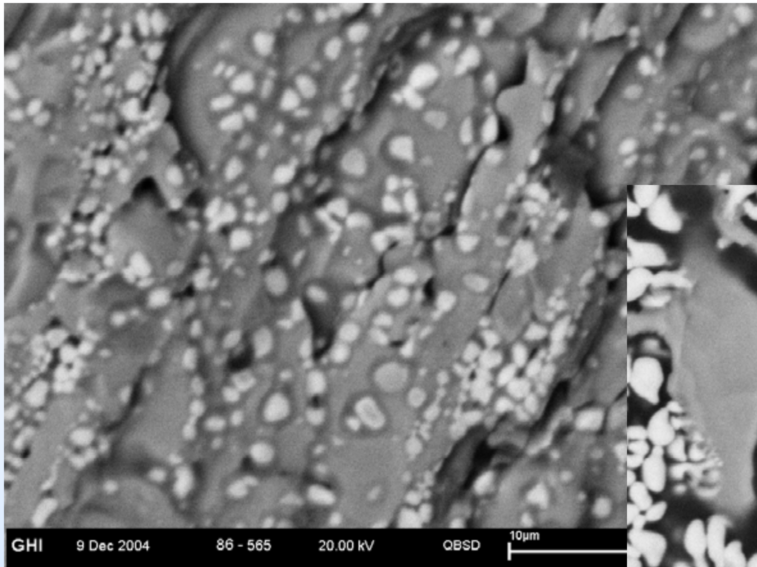

1660 °C / 0 h

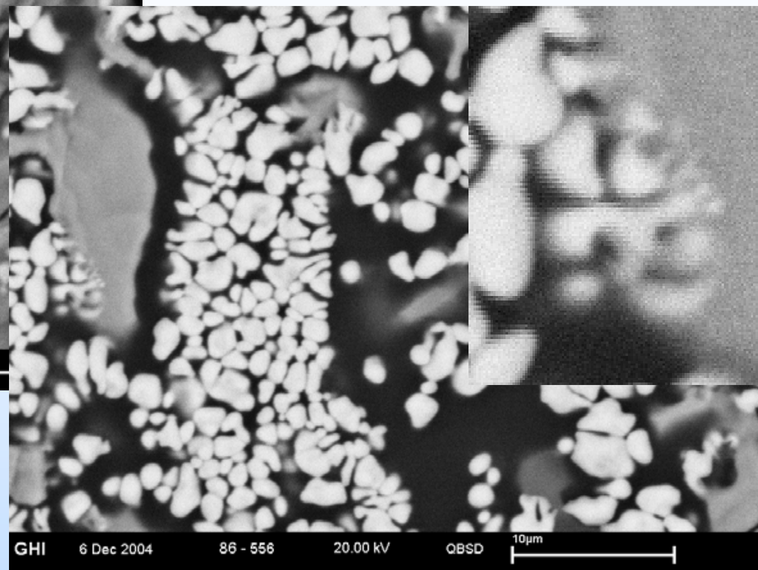

1680 °C / 0 h

Eutectic microstructure:
ZrO_2 + SiO_2-melt (~5 at.-% Zr)

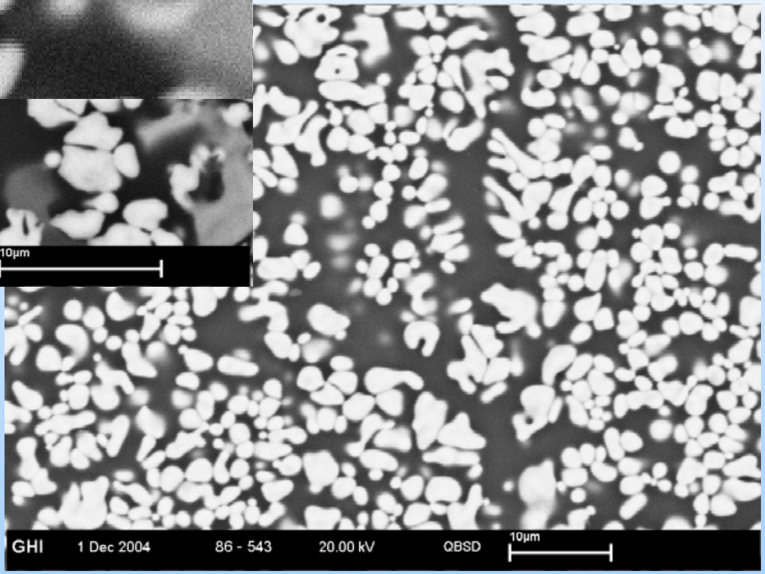

1700 °C / 1h

- $ZrSiO_4$ decompositon → solid state reaction
- multiple-stage process : demixing and gradual enrichment of SiO_2
  → discrete metastable, intermediate compounds
  → simultaneously precipitation of zirconia

Literature Review : Thermal Decomposition of $ZrSiO_4$

Author	Year	Decomposition of $ZrSiO_4$	Temperature
Washburn & Libman	1920	congruent melting	2550°C
Zhirnowa	1934	congruent melting	2430°C
Geller & Lang	1945	incongruent melting	1775°C
Curtis & Sowman	**1953**	solid state dissociation	**1540°C**
Toropov & Galakhov	**1956**	solid state dissociation	**1540°C**
Cocco & Schromek	1958	incongruent melting	1720°C
Rosén & Muan	1965	solid state dissociation	1600–1650 °C
Butterman & Foster	**1967**	solid state dissociation	**1676°C**
Jones, Kimura & Muan	**1967**	solid state dissociation	**1675 ± 10 °C**
Wecht	1972	solid state dissociation	1640 °C
Anseau, Biloque & Fierens	**1976**	solid state dissociation	**>1525-1634°C**
Fischer, Janke & Schulenburg	1976	solid state dissociation	1650-1680 °C
Klute & Woermann	**1982**	solid state dissociation	**1681 ± 5 °C**
Kanno	**1989**	solid state dissociation	**1650-1700°C**
Pavlik & Holland	2001	solid state dissociation	1258 °C
Levin	2001	solid state dissociation	1550 °C
O´Neill	**2003**	solid state dissociation	**1667 °C**

$T_{dissociation}$= 1673°C ± 10°C

$T_{eutectic}$= 1687°C ± 10°C

Thermodynamic Data

$\Delta H^0_{f,oxides,298}$ $[kJ/mol]$	$\Delta H^0_{f,elementes,298}$ $[kJ/mol]$	$S^0_{f,oxides,298}$ $[J/K \cdot mol]$	Source
-2023.801		84.027	BAR89
-2400.0 ± 20			O´NE01
-2034.2 ± 3.1		84.026	ELL92
-2035.7		84.027	KNA91
-2035.098 ± 8.4		84.5168	KUB79
		84.5168 ± 1.3	KUB67
-2023.956		83.87	CHA85
-2033.4		84.03	ROB78
-2022.1272		84.5168	MAT69
	-1917.54 ± 1.25		FER02
	-1918.47 ± 1.49		HOL98
	-2033.21 ± 1.1		MAN03
-2028.1412816		84.027272	FACTBASE FACT53BASE FToxidBASE

Calculated Phase Diagram ZrO_2-SiO_2

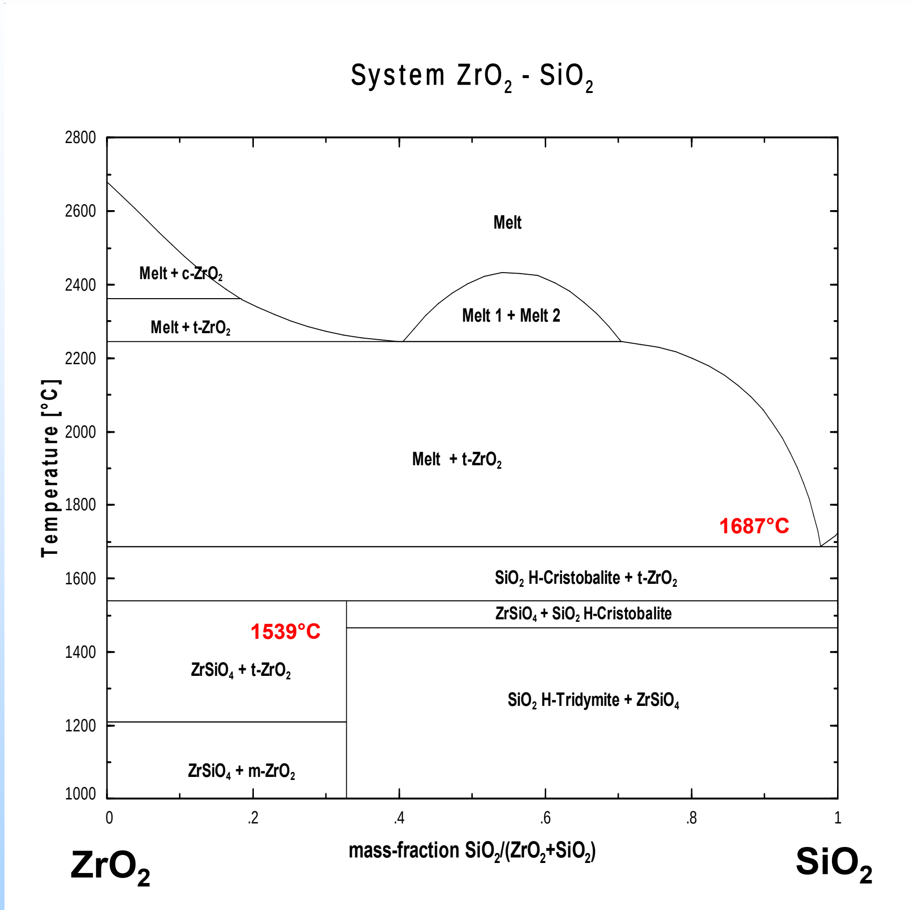

FactSage 5.5

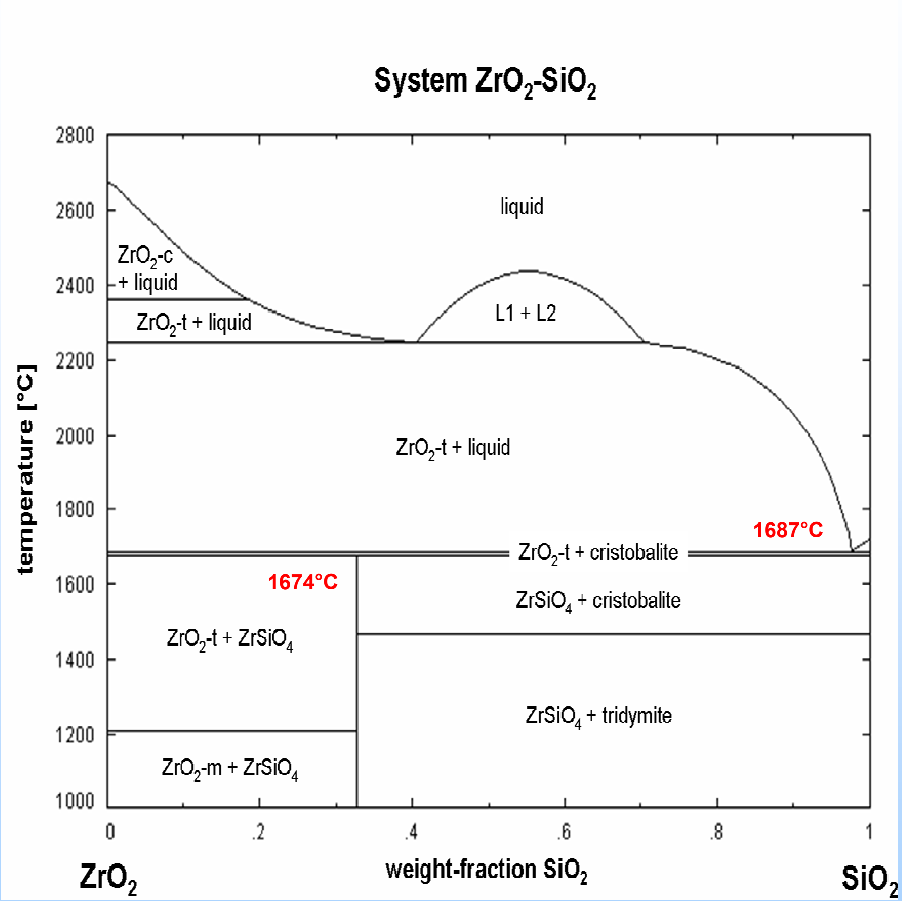

New Dataset

Calculated Phase Diagram ZrO_2-SiO_2

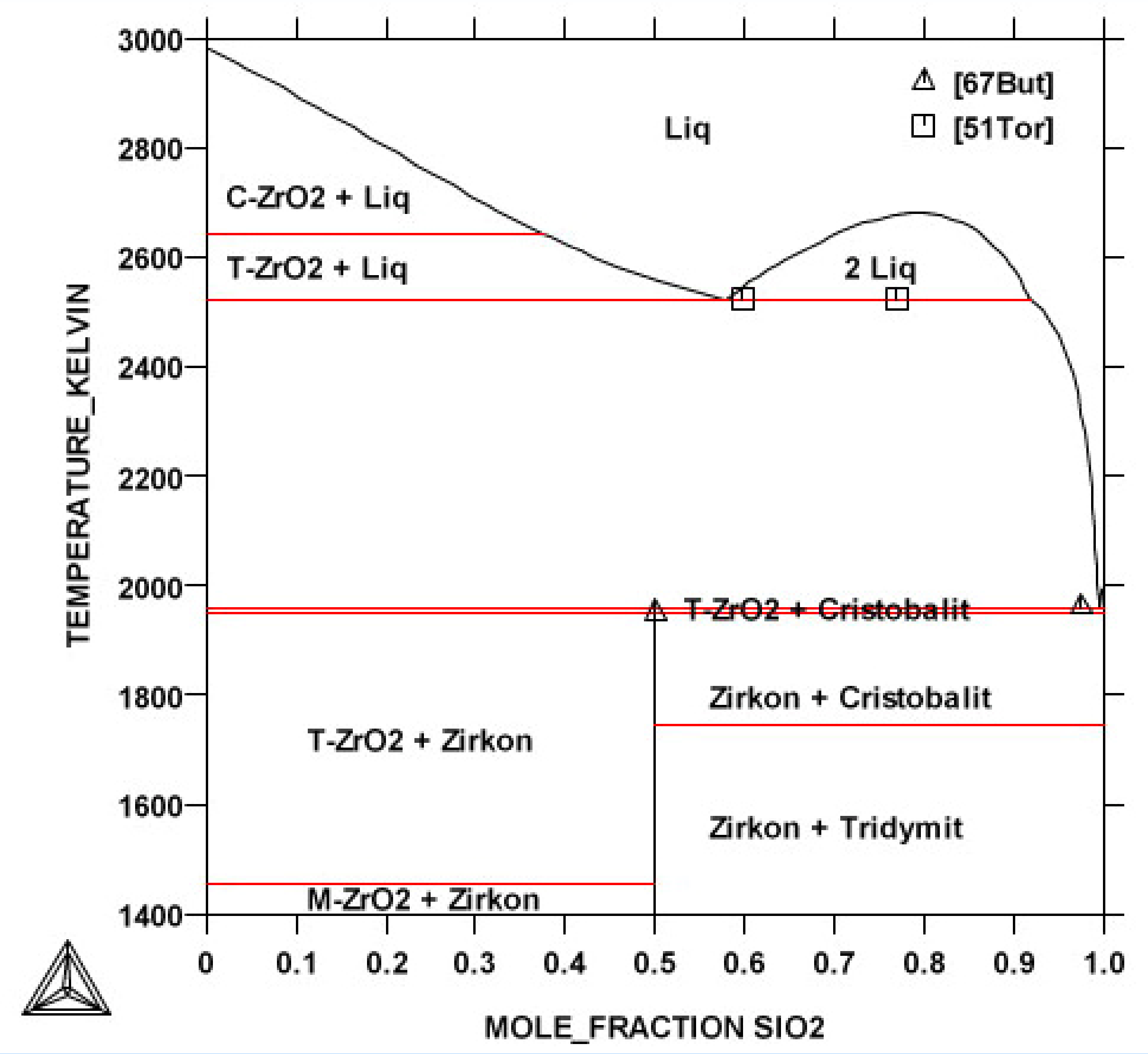

Calculated Phase Diagram ZrO_2-SiO_2

$T_{dissociation}$= 1673°C ± 10°C

$T_{eutectic}$= 1687°C ± 10°C

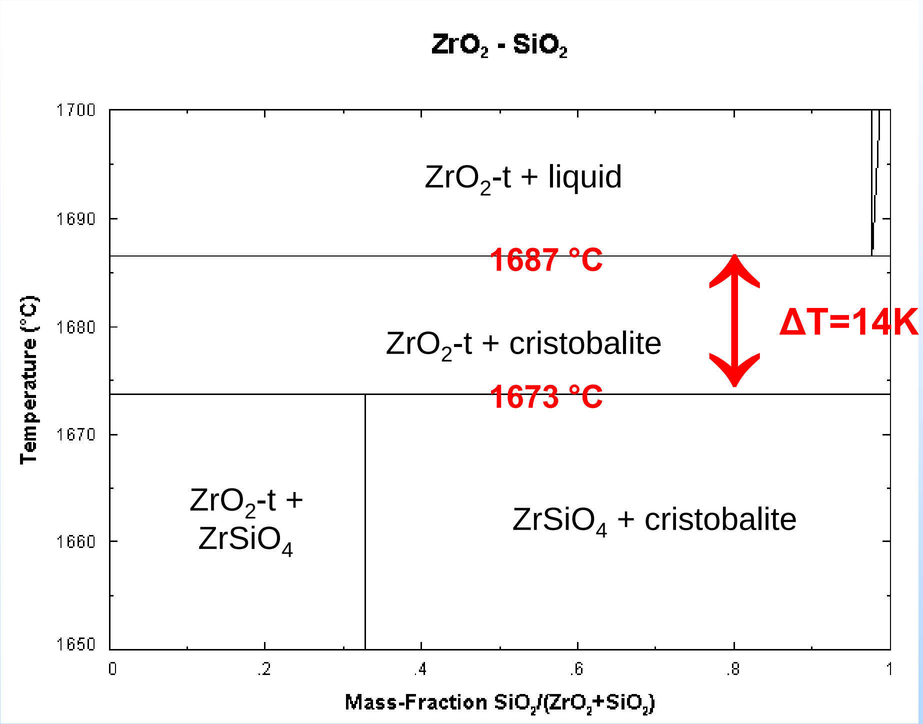

Impurites in natural zircon raw materials : rutile, illmenite, magnetite, quartz, corundum, kyanite, …

ΔT = 14K → Degradation of eutectic temperature in the binary system below the solid state dissociation temperature even by minor impurities

→ Solid state dissociation superimposed by formation of a silicate melt at temperatures noticeable below the dissociation temperature

Thermal Decomposition of Natural Zircon Raw Materials

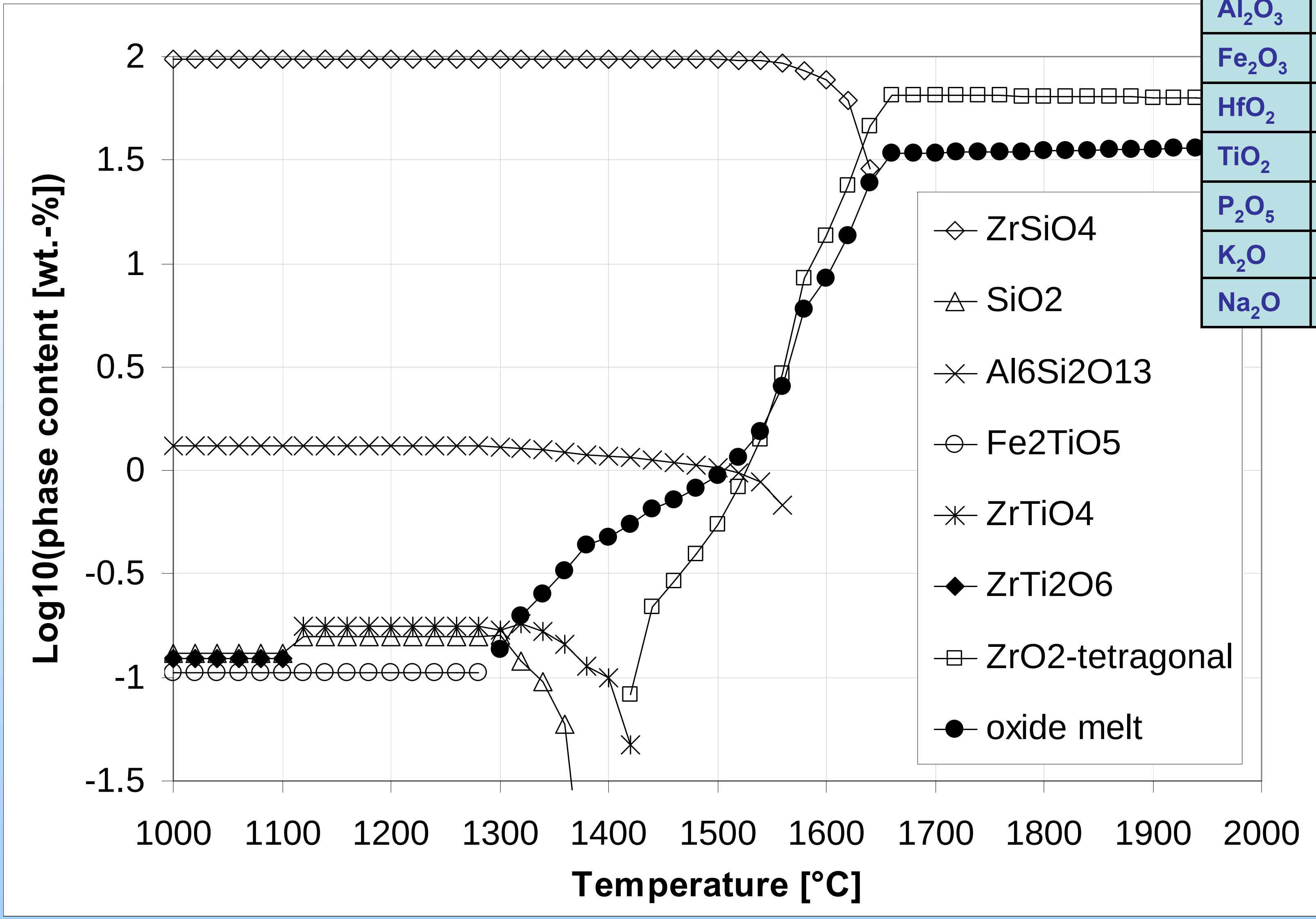

	Gew.-%
Al_2O_3	0.94
Fe_2O_3	0.063
HfO_2	in ZrO_2
TiO_2	0.105
P_2O_5	0.111
K_2O	-
Na_2O	-

Thermal Decomposition of Natural Zircon Raw Materials

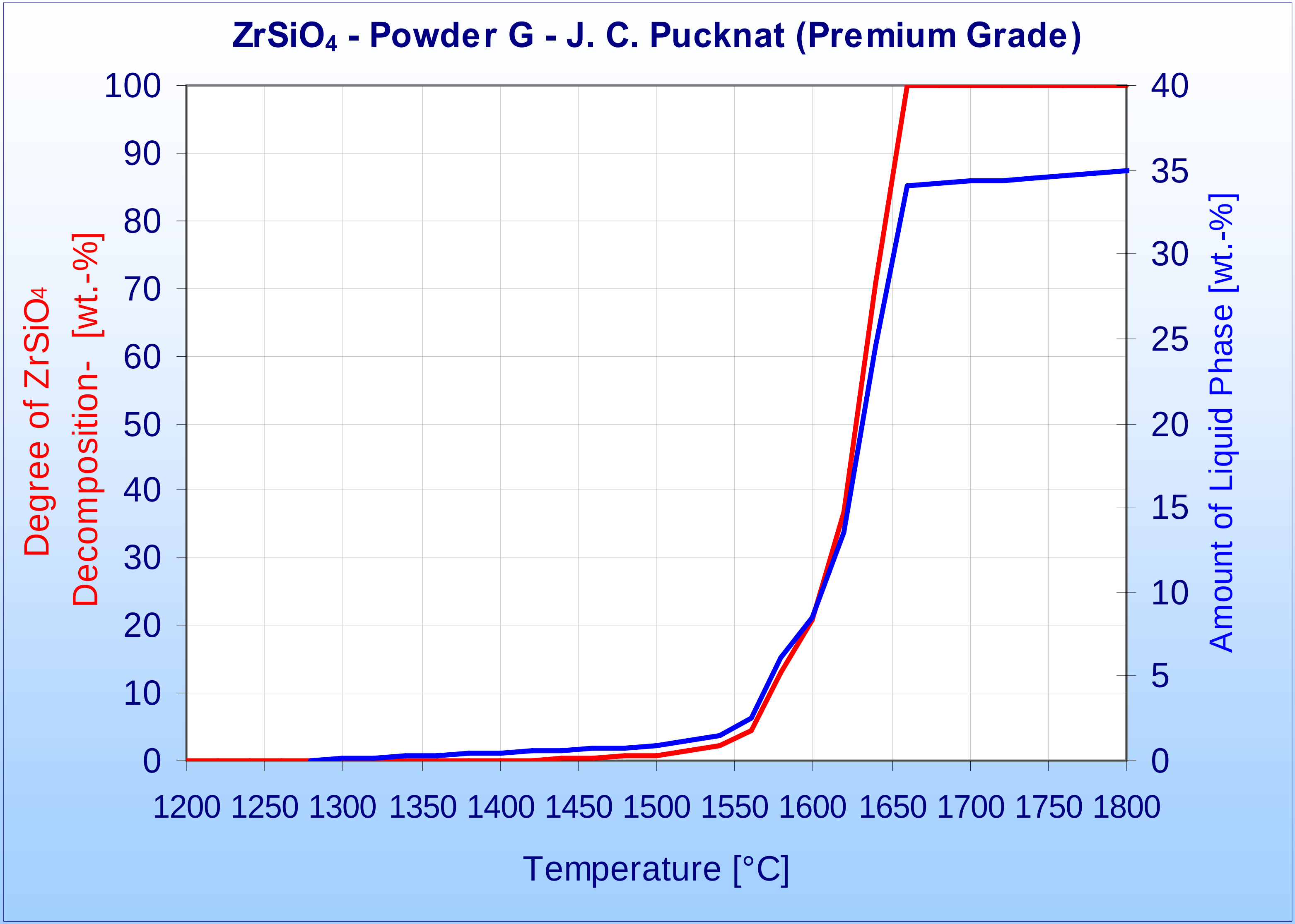

Thermal Decomposition of Natural Zircon Raw Materials

Anseau, Biloque & Fierens (1976)

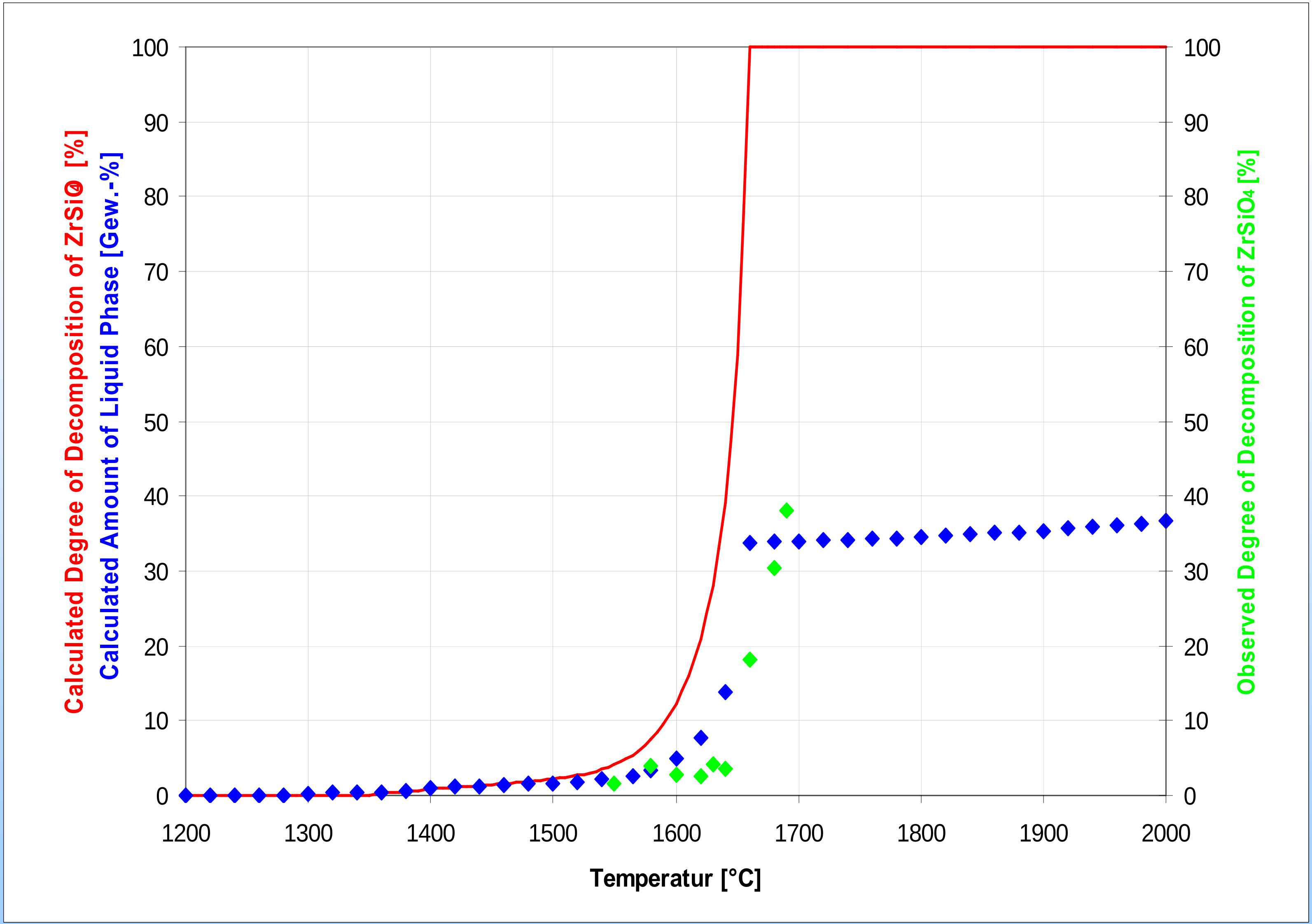

Thermal Decompositon of Natural Zircon Raw Materials

$ZrSiO_4$-Powder G (U. C. Pucknat)

1600 °C / 16h / quenching

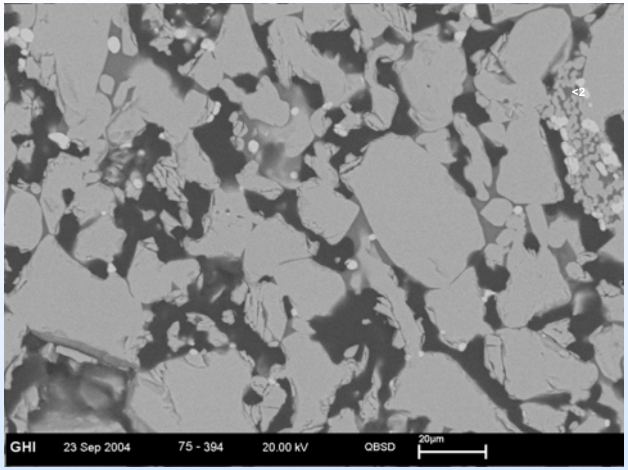

1650 °C / 16h / quenching

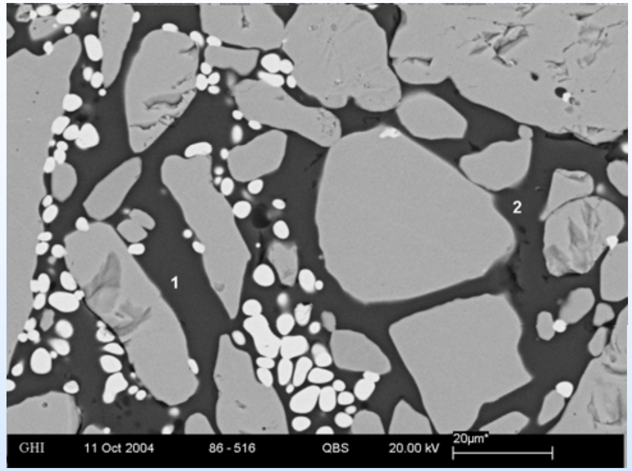

1700 °C / 5h / furnace cooled

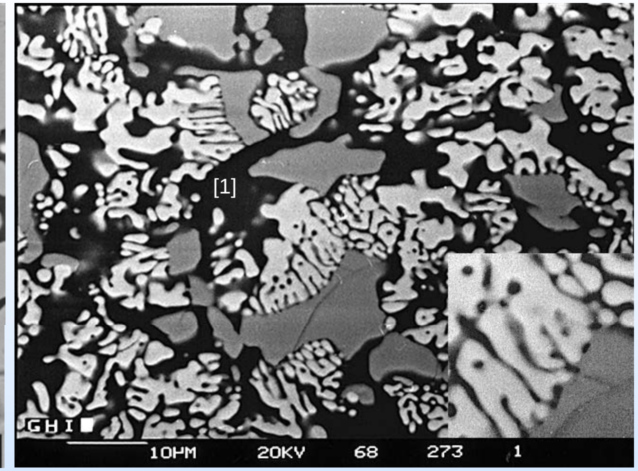

	Gew.-%
Al_2O_3	0.94
Fe_2O_3	0.063
HfO_2	in ZrO_2
TiO_2	0.105
P_2O_5	0.111
K_2O	-
Na_2O	-

Impurities Raw Material

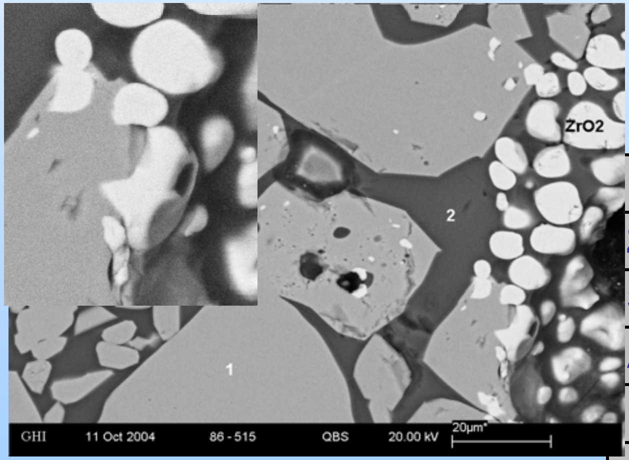

Melt Composition:

	1600	1650	1700
ZrO_2	8.93	8.86	13.5
SiO_2	64.80	78.04	81.1
Al_2O_3	20.76	10.12	5.4
Fe_2O_3	2.56	1.08	-
TiO_2	2.95	1.89	-

Thermal Decomposition of Natural Zircon Raw Materials
Mineral Impurities: Rutile, Ilmenite, Magnetite, Corundum, Quarz, Kyanite, …

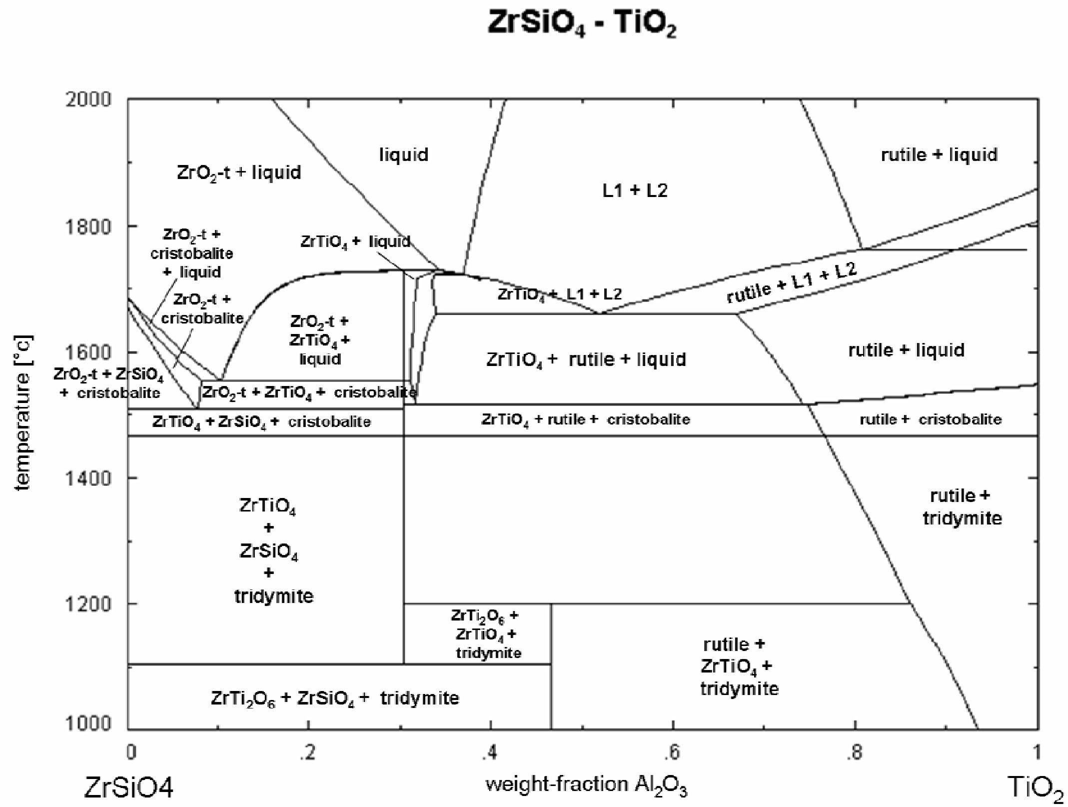

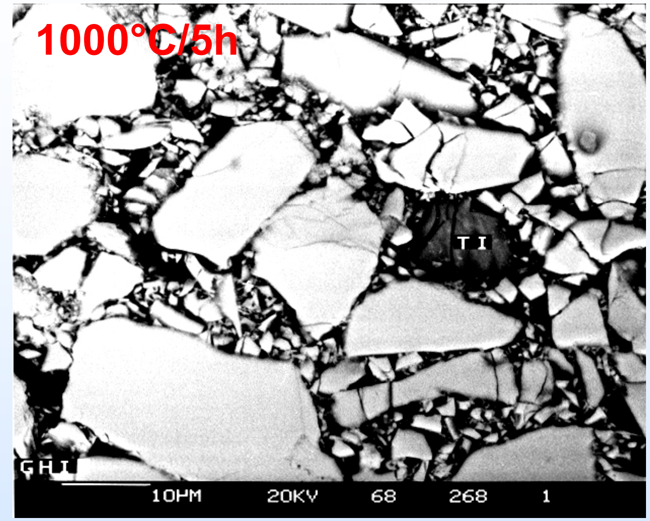

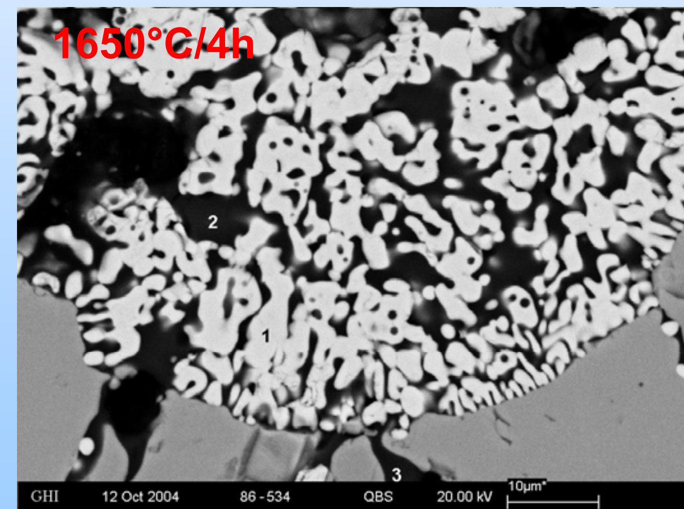

[1]: ZrO_2 – grain with 5.70 wt.-% TiO_2

[2]: SiO_2-TiO_2-melt between ZrO_2-grains (81.81 wt.-% SiO_2, 3.61 wt.-% Al_2O_3, 9.39 wt.-% TiO_2, 5.19 wt.-% ZrO_2

Thermal Partial Oxidation Process for Fuel-Cell Anode Gas Synthesis

Advantages of Thermal Partial Oxidation:

- non-catalytical process (costs; toxicity)
- reforming of all liquid hydrocarbons (sulfur concentration, aromatics content)
- no external heat source
- educt conditioning: air, liquid hydrocarbons

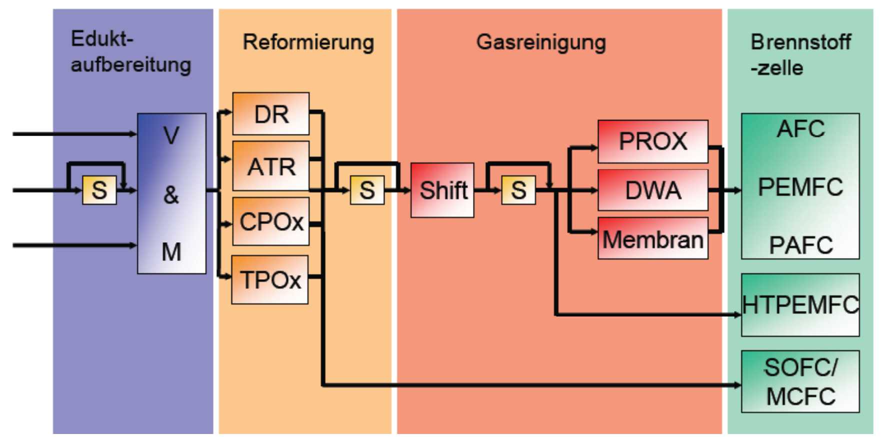

S = Entschwefelung, V = Verdampfung, M = Mischen

Inert Porous Ceramic Structures for Thermal Partial Oxidation:

- flame stabilization at high temperatures
- self-igniton of the air/hydrocarbon mixture at the ceramic matric
- higher combustion rate
- lower process temperatures → reduced NO_x
- lower noise emission

Thermal Partial Oxidation of Methane CH_4

$$CH_4 + \frac{1}{2} O_2 = 1\ CO + 2\ H_2$$

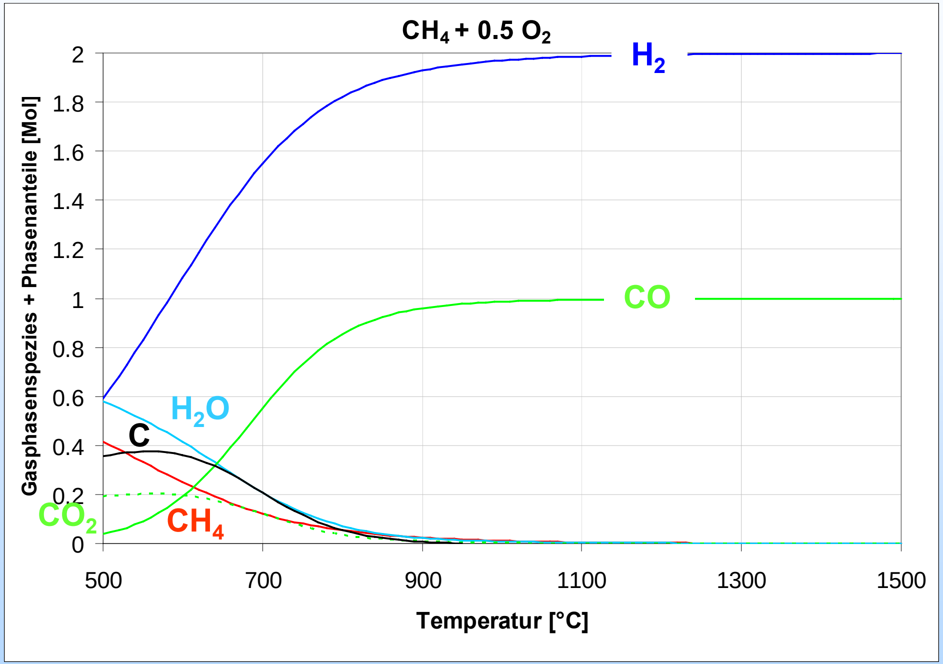

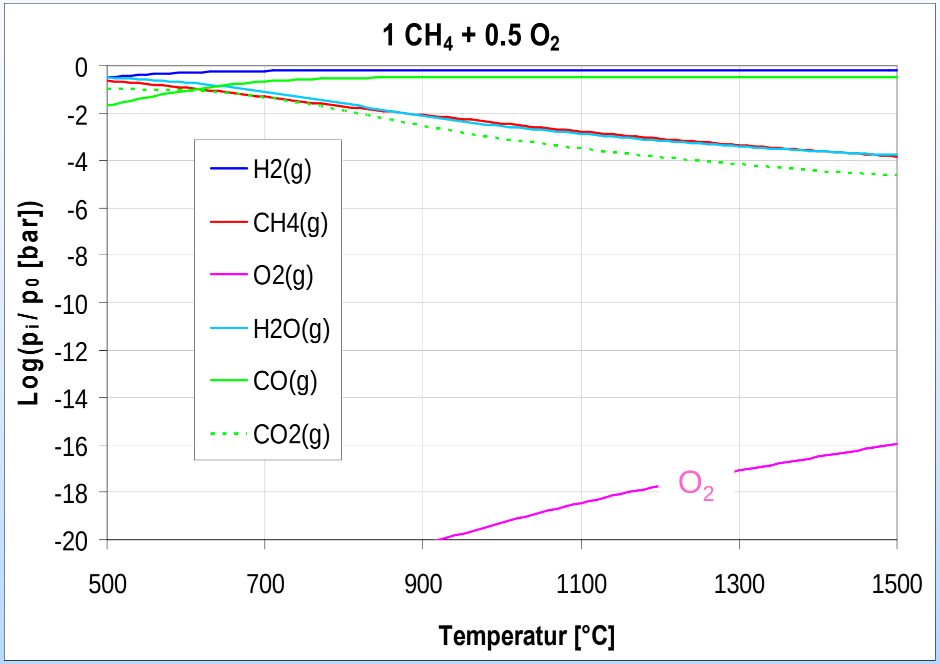

Thermal Partial Oxidation of Light Fuel Oil

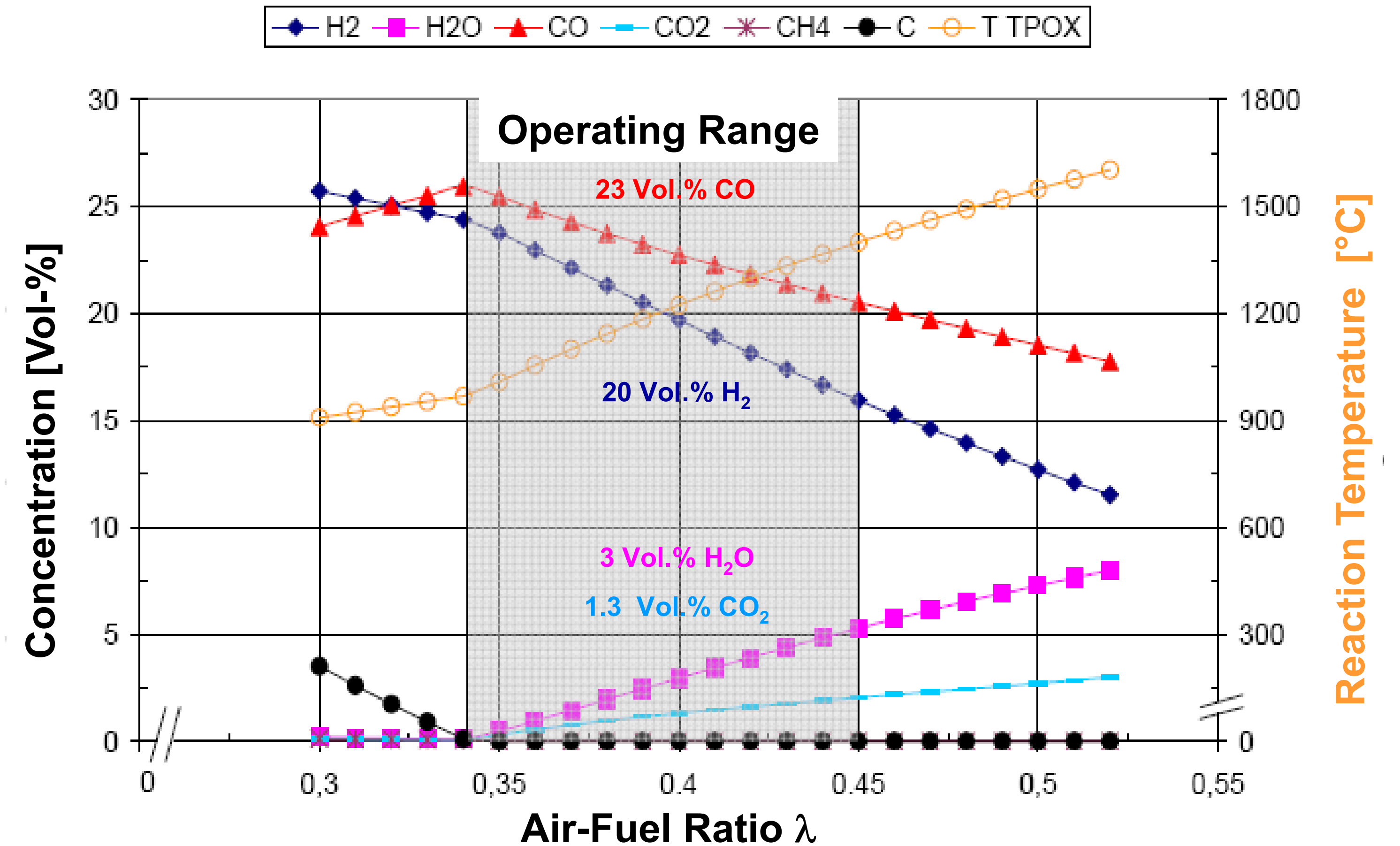

Equilibrium calculation for Fuel Oil EL (Amphlet Diesel) φ_{Inlet}=400°C, p=1bar

→ highly reducing atmospheres (+ carbon black formation at low temperatures)

→ oxidizing atmospheres in case of start-up and shut-down procedures

→ temperatures up to 1500°C

Thermal Partial Oxidation of Light Fuel Oil

	[Vol.-%]	COS [ppmV]	H_2S [ppmV]			[µg/kg]
	λ=0.45, 1200 °C, 1bar					
CO	23				B	100
H_2	20				Pb	50
H_2O	3				Na	100
CO_2	1.3				Cl	500
N_2	52.7				Sn	50
					Ca	110
10 ppm S		0.1	1.5		Fe	60
100 ppm S		1	15		Si	118
150 ppm S		1.5	22.5			
1000 ppm S		10	150			
2000 ppm S		20	300			

Combustion of Heavy Fuel Oil / Steam - Mixtures

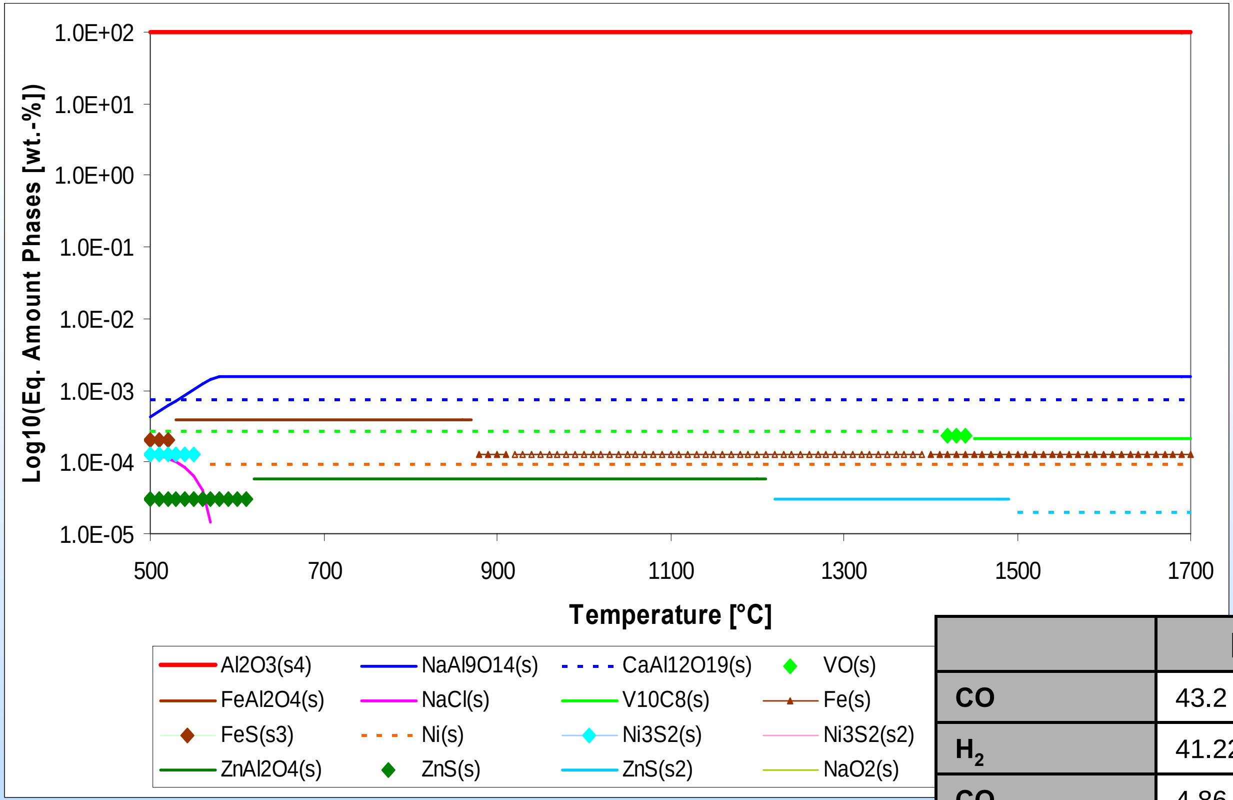

	[Vol.-%]		[mg/kg]
CO	43.2	Ca	11
H_2	41.22	Ni	23
CO_2	4.86	V	44
CH_4	0.18	Na	18
H_2S (COS)	0.54	Zn	5
H_2O	10	Fe	31
NH_3	50 ppm	Cl	17
Cl	< 10 ppm		
HCN	10 – 30 ppm		

Thermal Partial Oxidation of Light Fuel Oil
1000 ppm S

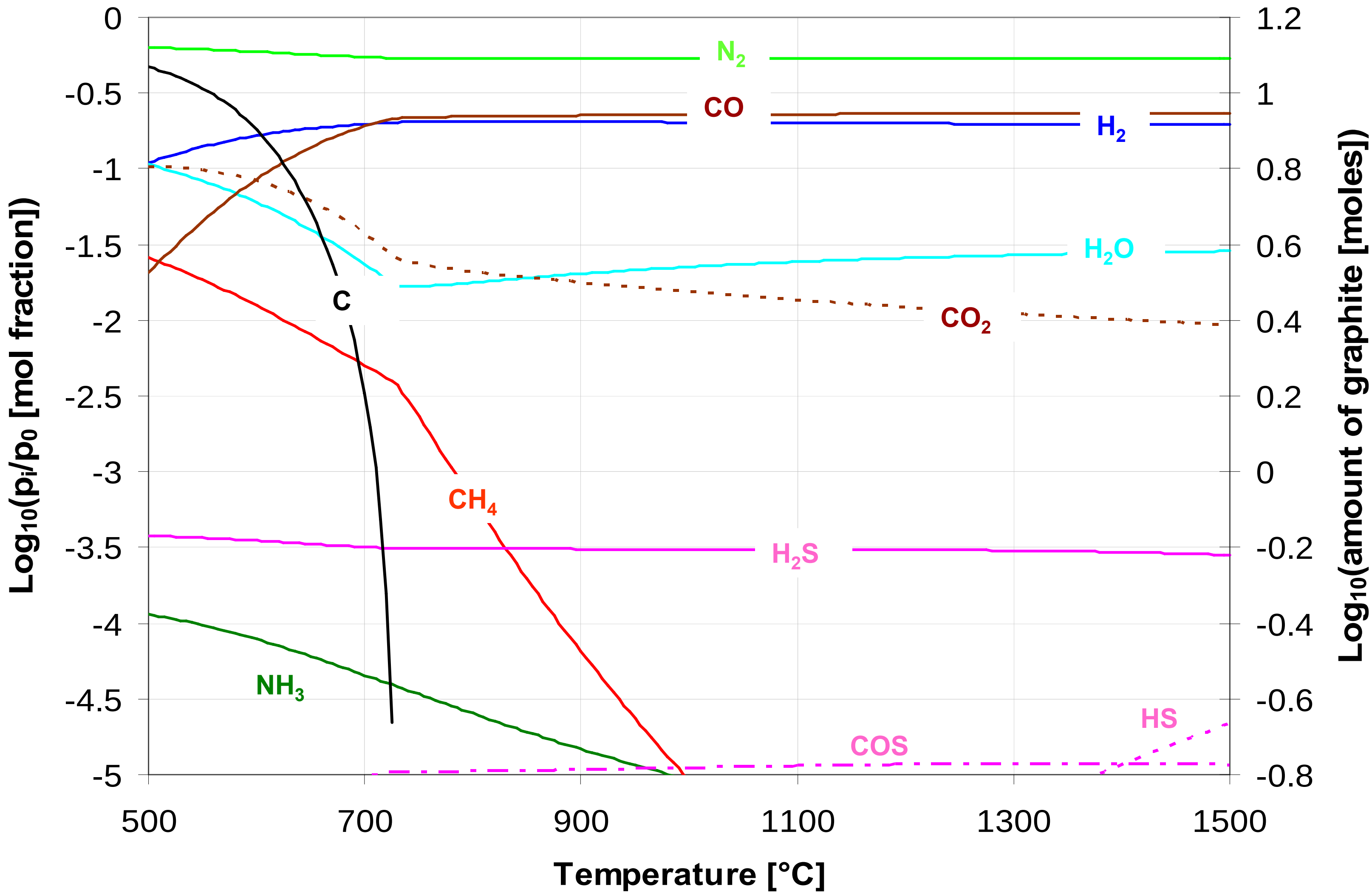

Materials Selection: Heat Capacity ↓, Emissivity ↑, Thermal Shock Resistance ↑
→Thermal and Chemical Stability in Oxidizing, Reducing (Boudouard) and Syngas Atmospheres

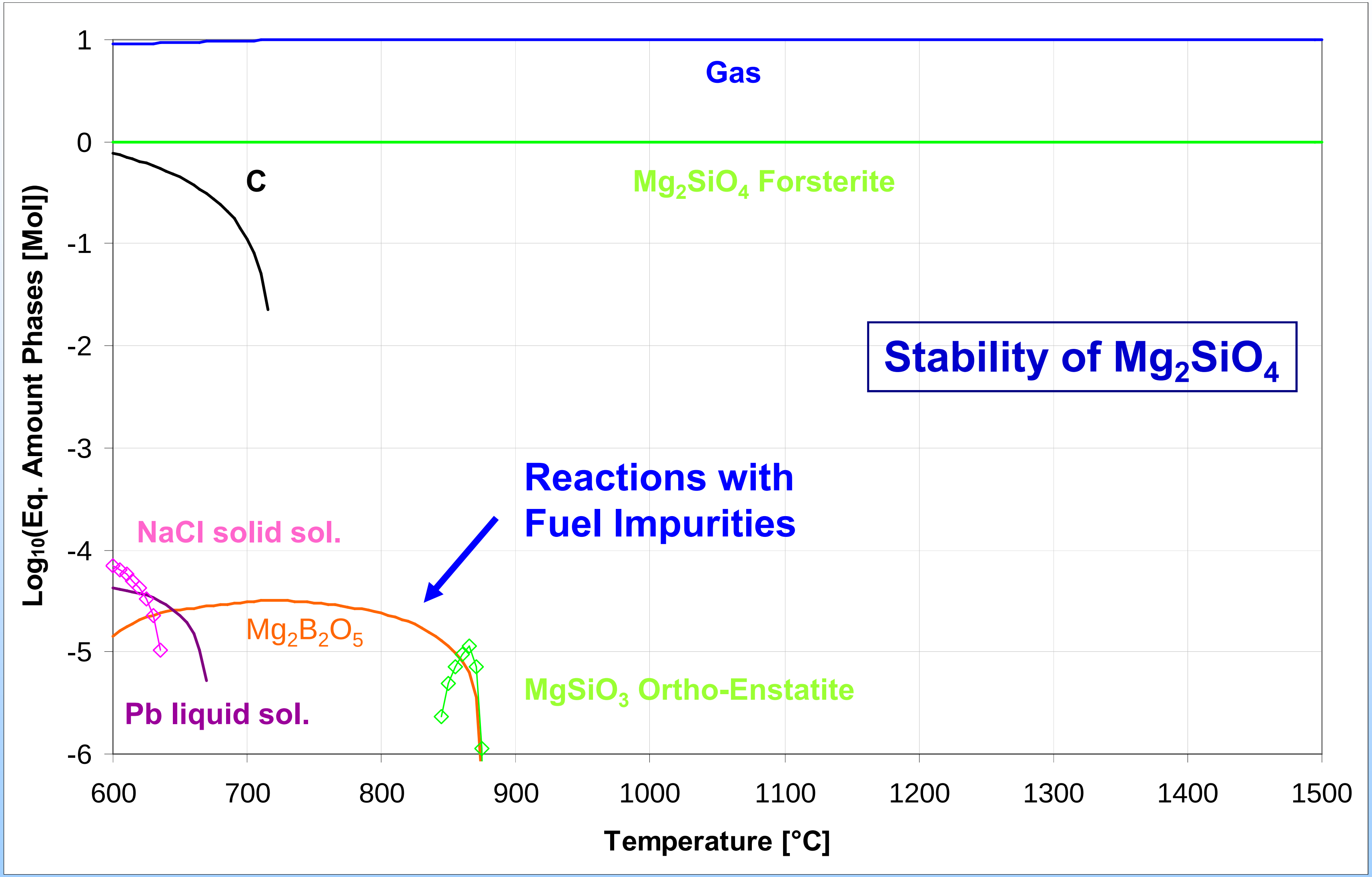

Thermal Partial Oxidation of CH_4 – Stability of $CaAl_2SiO_6$

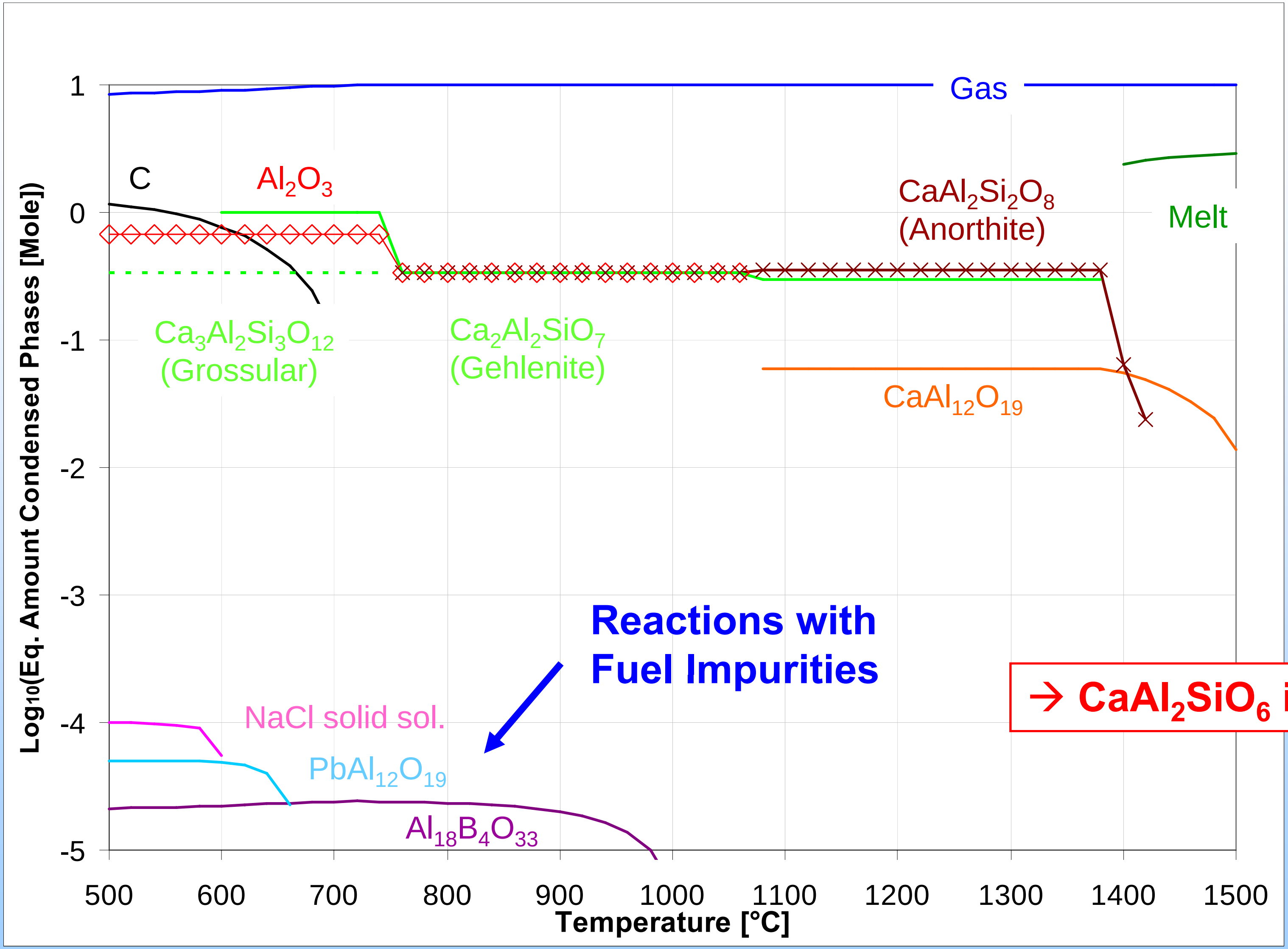

→ $CaAl_2SiO_6$ instable

Thermal Partial Oxidation of CH_4 – Stability of SiC

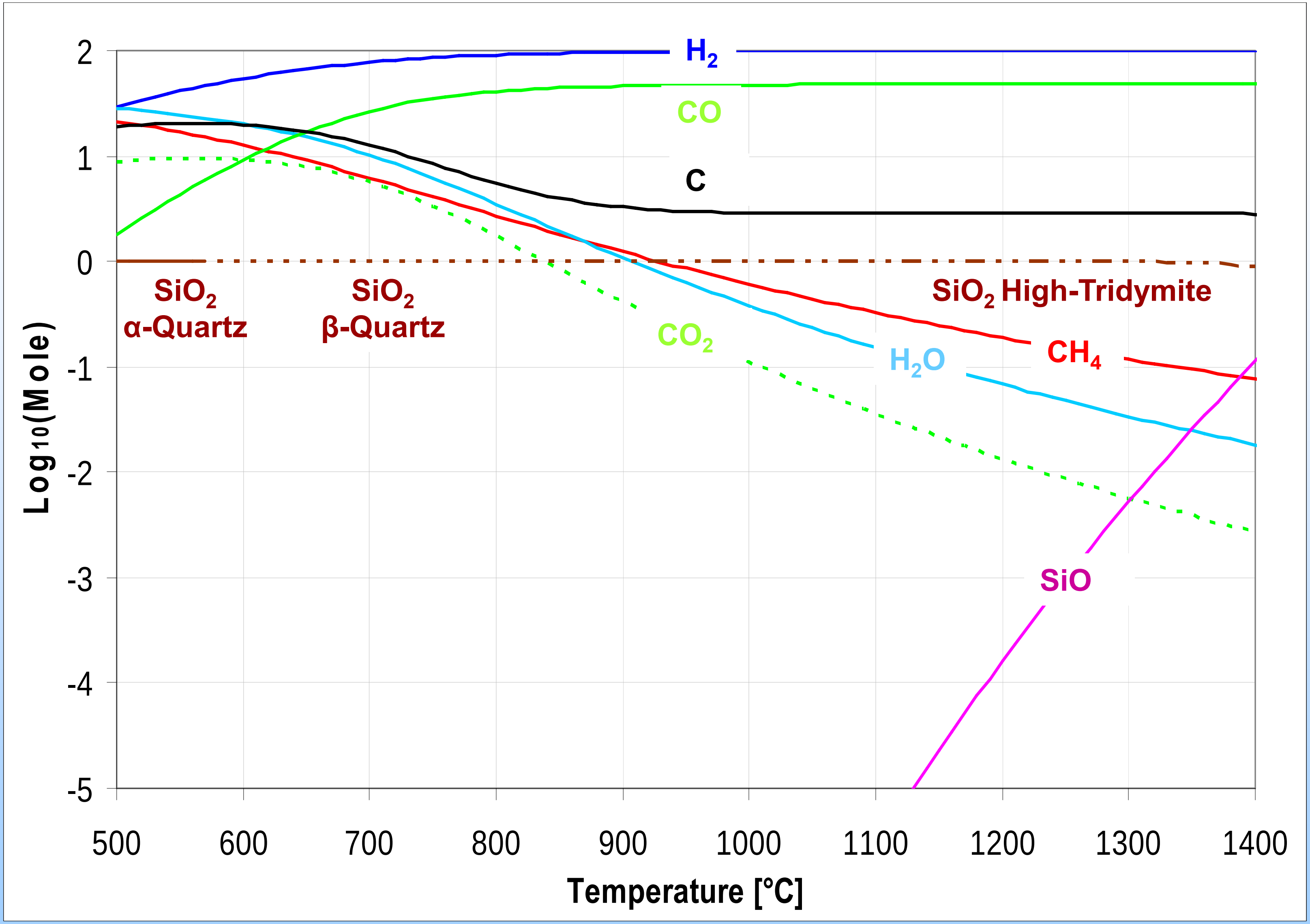

Thermal Partial Oxidation of CH_4 – Stability of Si_3N_4

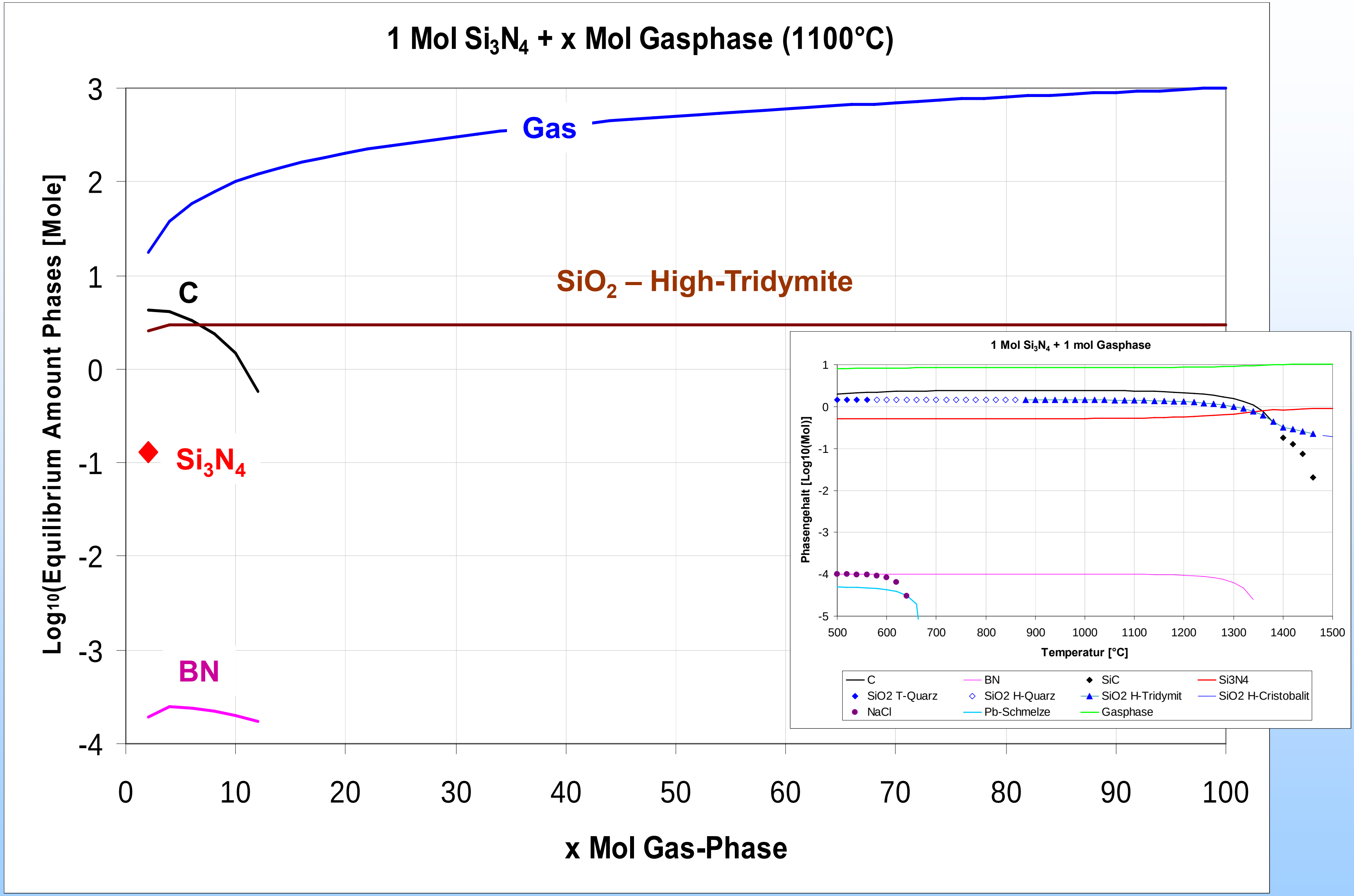

Thermal Partial Oxidation of Light Fuel Oil

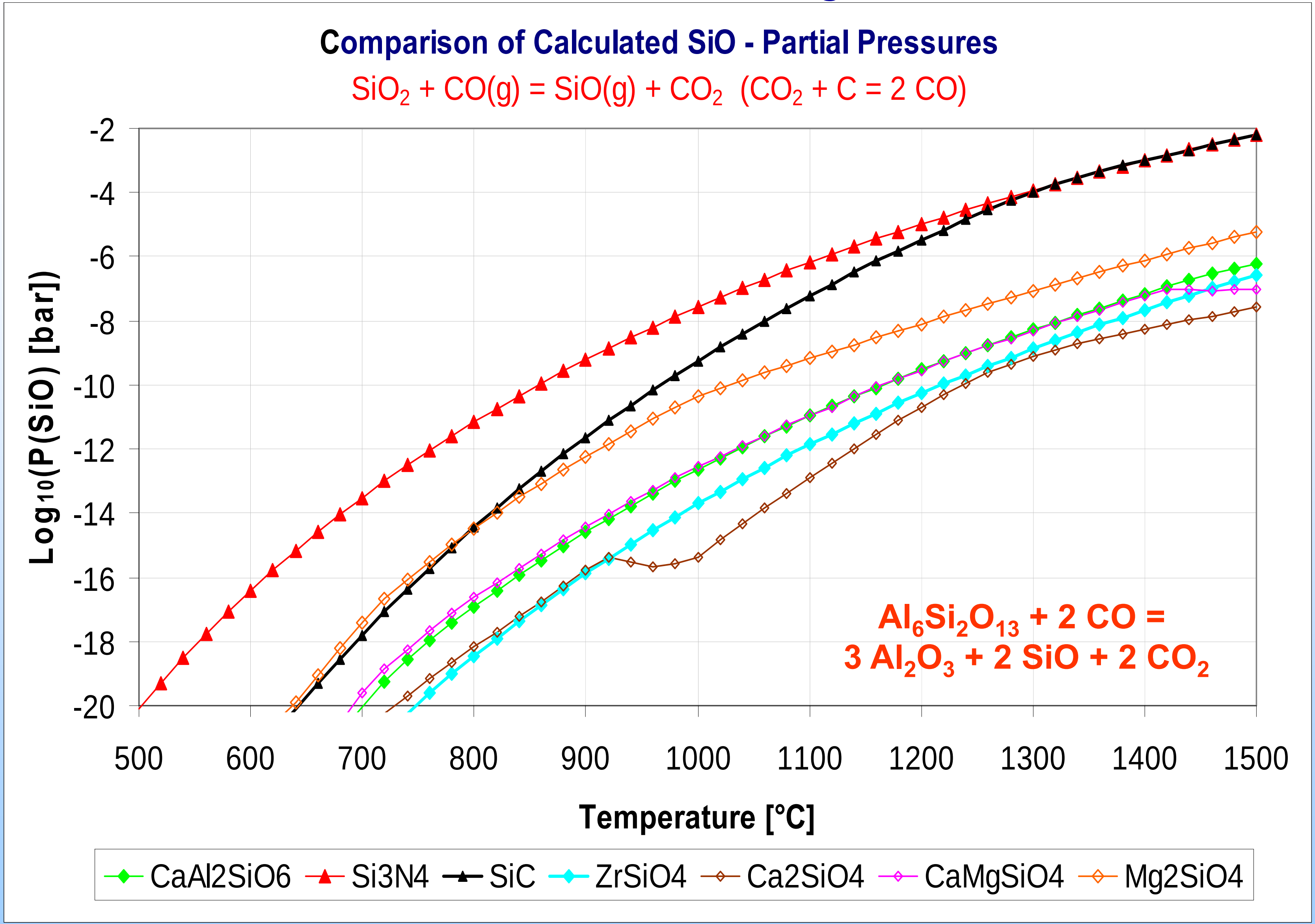

Thermal Partial Oxidation of Light Fuel Oil – Stability of $ZrTiO_4$

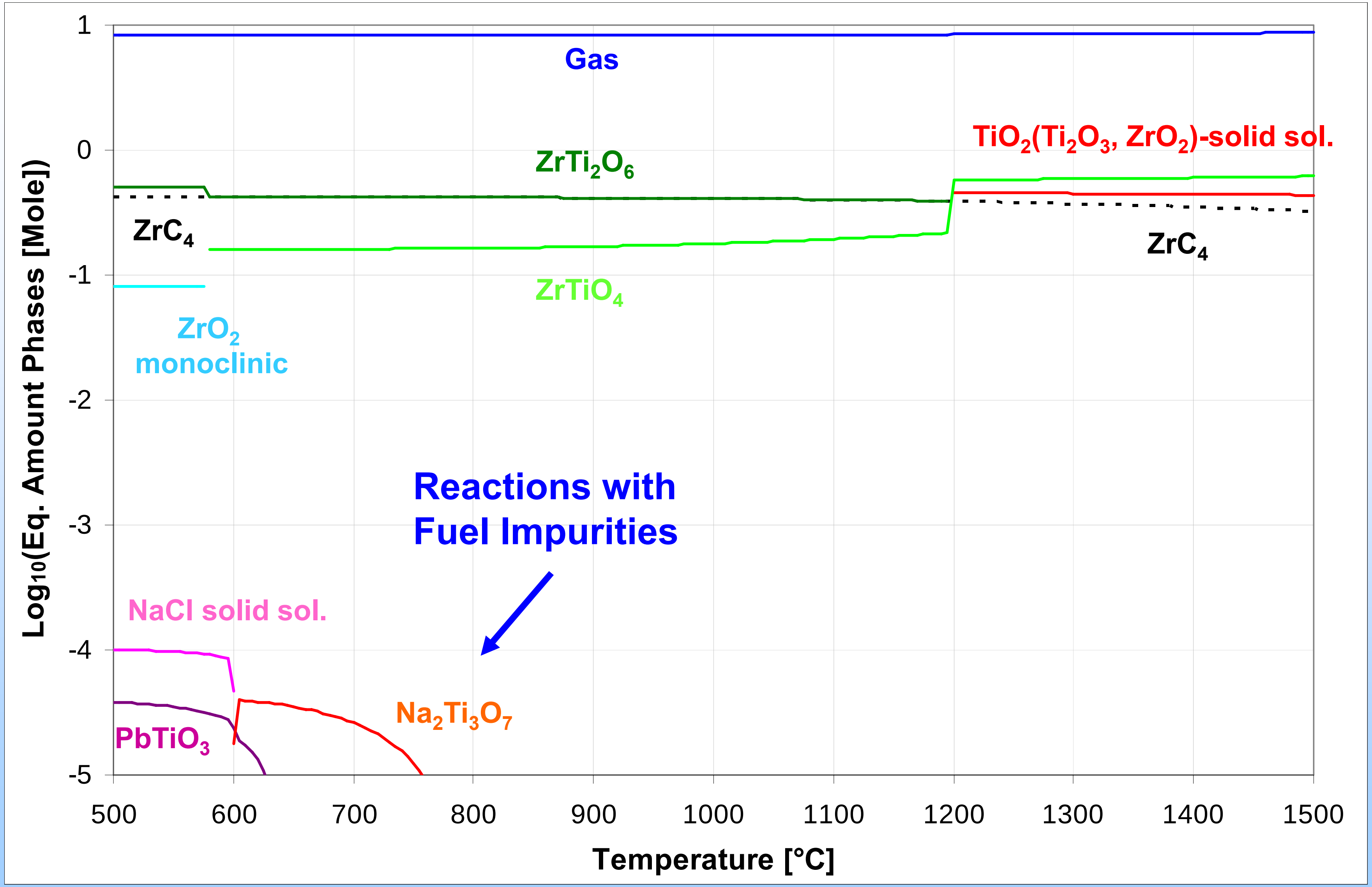

Thermal Partial Oxidation of Light Fuel Oil – Stability of $ZrTiO_4$

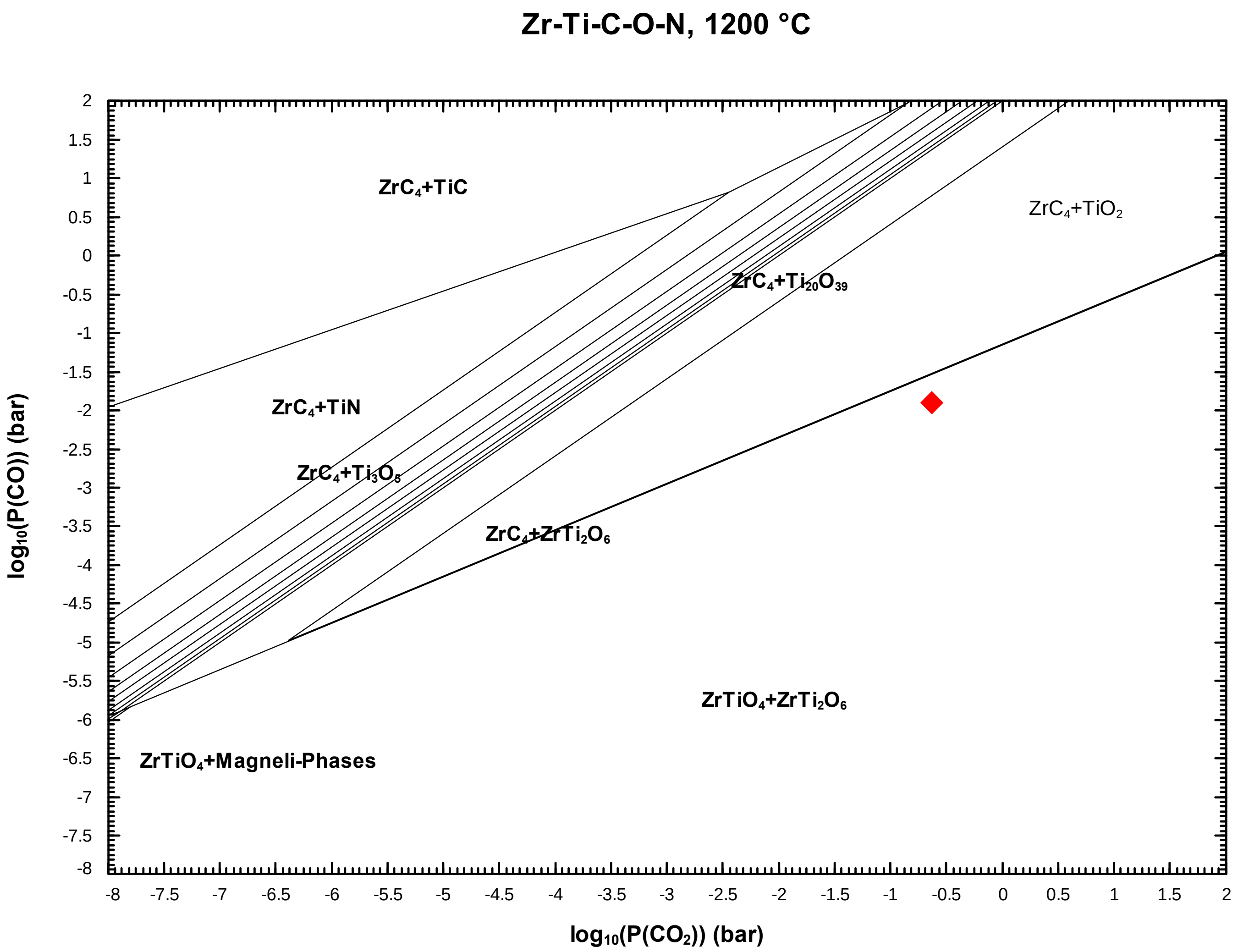

Thermal Partial Oxidation of Light Fuel Oil – Stability of $MgTiO_3$

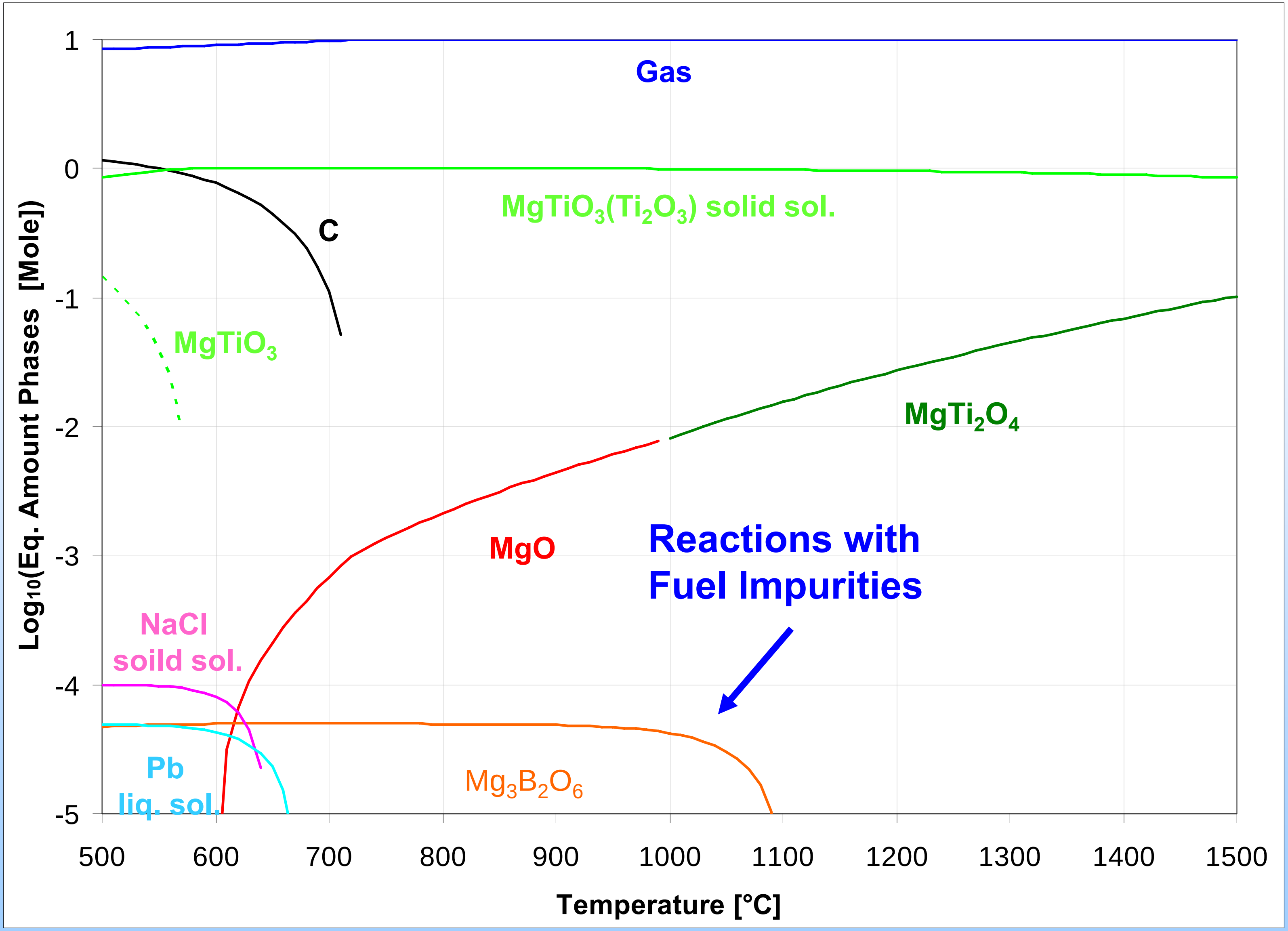

Thermal Partial Oxidation of Light Fuel Oil

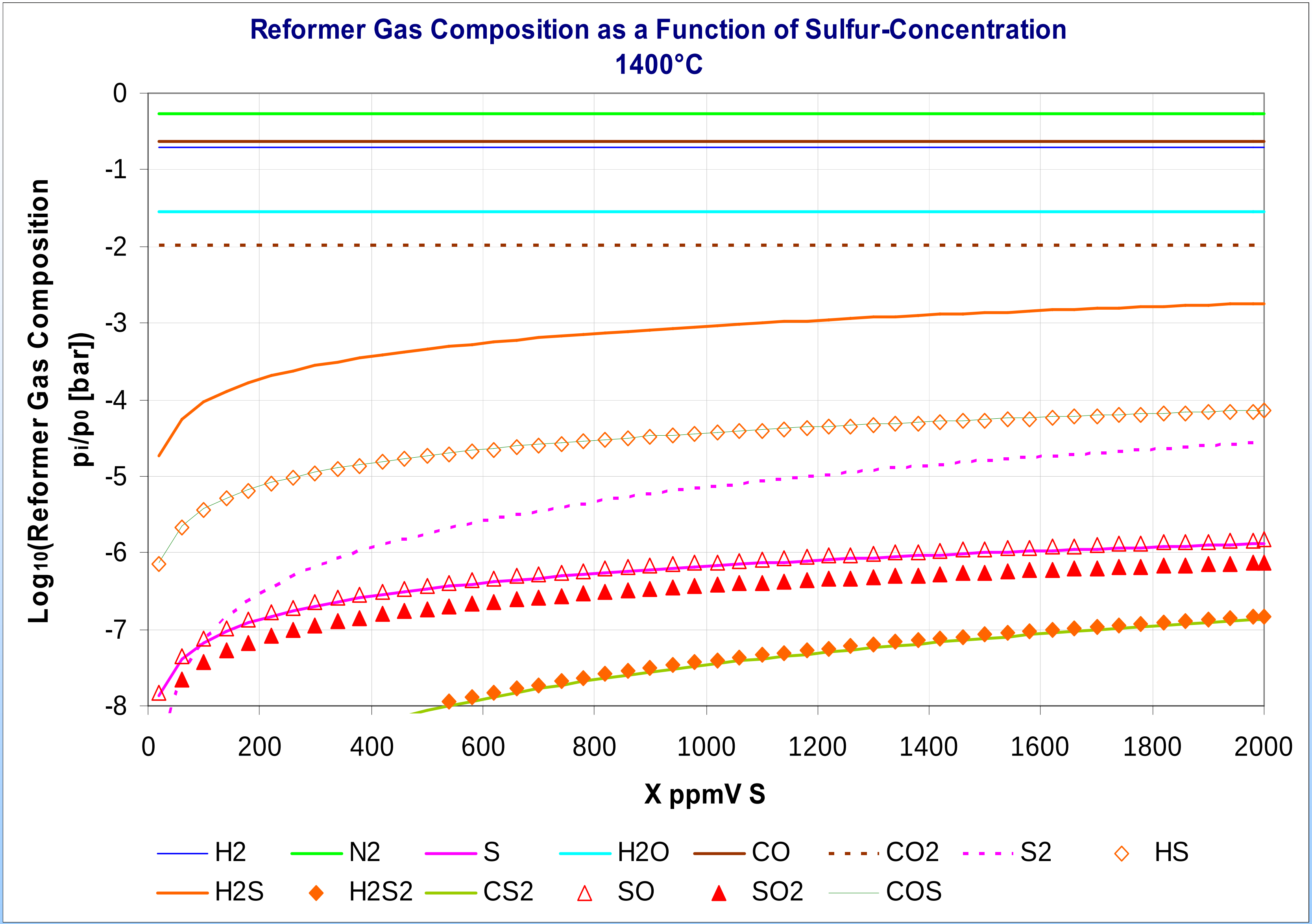

Thermochemical Calculations
Applied to High Temperature Corrosion
of Ceramic and Refractory Materials

RWTH AACHEN UNIVERSITY

Thermal Partial Oxidation of Light Fuel Oil

Effect of Sulfur Concentraion in the Fuels

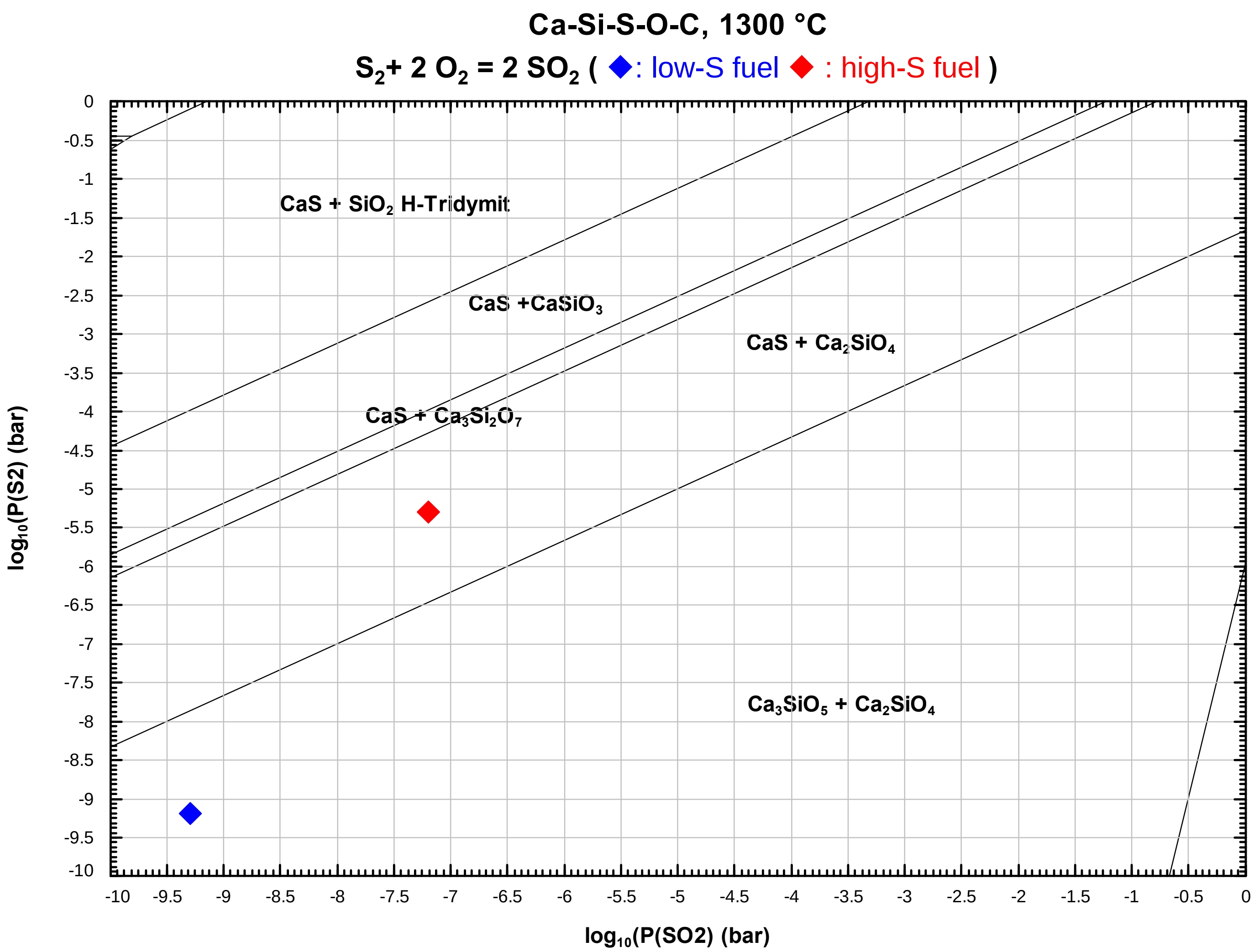

Thermal Partial Oxidation Process for Fuel-Cell Anode Gas Synthesis

Materials Selection:

$CaAl_2O_4$, Mg_2SiO_4, $NdAlO_3$, …

Foam Ceramics

tPOX-Reactor:

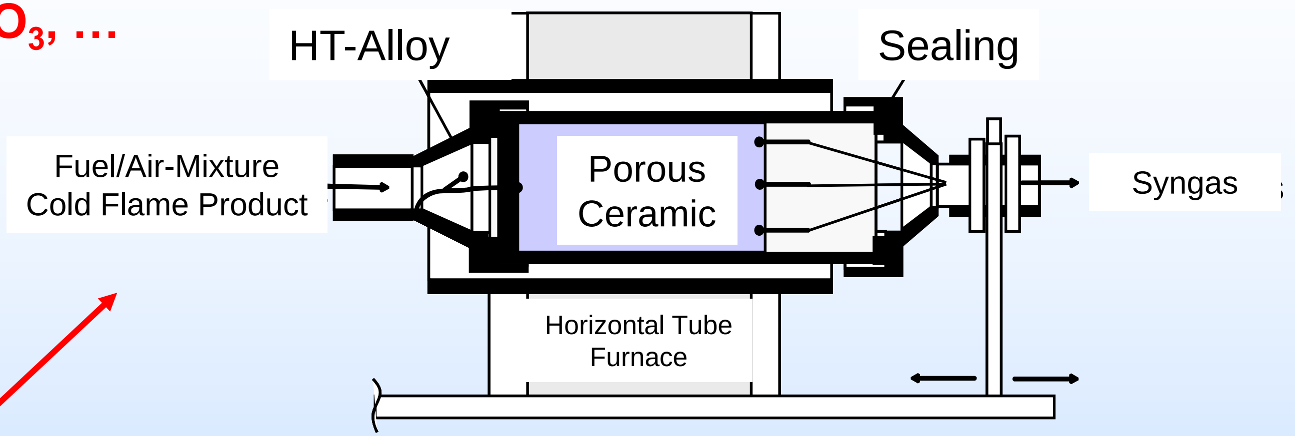

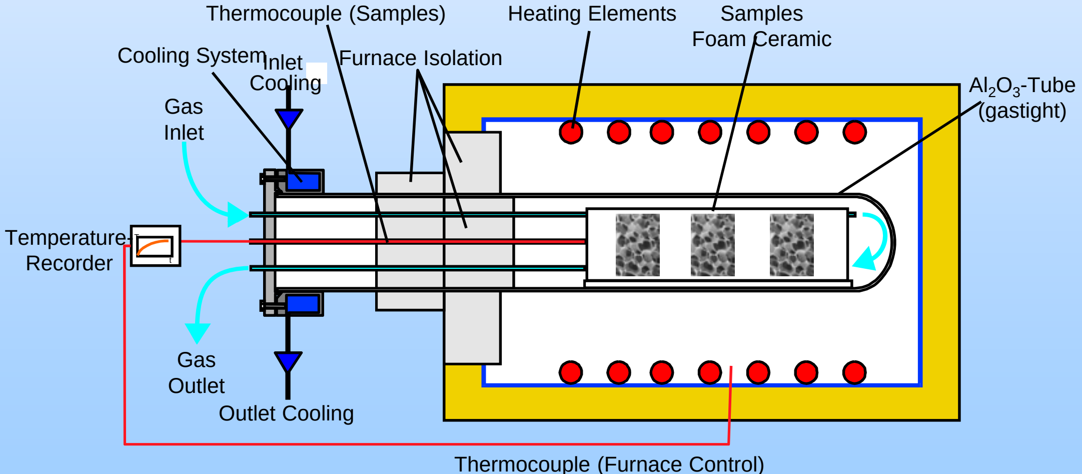

Gas Phase Corrosion Tests:

- Components (CO, CO_2, H_2, H_2O)
- Boudouard-Equilibrium
- Formier-Gas Atmosphere
- Gasmixtures for Simulation of Syngas-Atm.
- T_{max} = 1400 °C, 1 bar